Galerkin Least Square FEM for the European option price with CEV model

A Major Qualifying Project

Submitted to the Faculty of

Worcester Polytechnic Institute

In partial fulfillment of requirements for the

Degree of Bachelor of Science

By

Tuan Nhat Le

Date: January 24th, 2014

Advisor: Professor Marcus Sarkis

Abstract

For the evaluation of European options with constant local volatility, a general closed-form analytical solution was given by the classic Black-Scholes formula. In practice, such local volatility may vary, and in those situations, the Black-Scholes formula does not work efficiently. A common way to deal with such problem is to apply numerical methods, particularly the Finite Element Method (FEM). Furthermore, the extensive use of Galerkin Least Square (GLS) stabilization method combined with adaptive mesh refinements is explored for bad scenarios having large local volatility. Such local volatility was described by the Constant Elasticity of Variance (CEV) model. We implement our numerical schemes in Matlab and observe the accurracy of our numerical solutions. Finally, we take advantage of better ways to discretize our domain with geometric partition to achieve high accuracy despite of large local volatility.

Keywords: Option, Black-Scholes equation, Finite Element Method, Hat function, Hilbert space.

Contents

List of Figures

List of Tables

Acknowledgement

I want to dedicate special thanks to Professor Marcus Sarkis for his carefully weekly guidance, his continual support and his availability throughout the four terms. I am very grateful to receive his recommendation for an interesting book and good problems that he brought up in most of our meetings. Without his help, this project would not be possible.

1 Introduction

In our financial world nowadays, option is a very important financial instrument used for hedging, arbitrage-free investing and highly speculative trading by giving the buyer the right to buy (call) or sell (put) a security or other financial asset at an agreed-upon price (the strike price) during a certain period of time or on a specic date (exercise date). The three most popular types of options are European, American, and Asian options. For this project, we only concern about the pricing of European option. Pricing this type of option requires the use of Black-Scholes model, which assumes the price of a risky asset (underlying asset) is a solution to the stochastic differential equation:

$$ds = s(\tilde{r}_{\tilde{t}}d\tilde{t} + \tilde{\sigma}_{\tilde{t}}W_{\tilde{t}}) \tag{1}$$

where $W_{\tilde{t}}$ is a standard Brownian motion, $\tilde{\sigma}_{\tilde{t}}$ is a volatility, $\tilde{r}_{\tilde{t}}$ is an instantaneous interest rate, and s is a price of a risky asset at time $\tilde{t}$.

1.1 European Option

When $\tilde{\sigma}_{\tilde{t}} = \tilde{\sigma}_t(s, \tilde{t})$ and $\tilde{r}_{\tilde{t}} = \tilde{r}(\tilde{t})\,(0 \leq \tilde{t} \leq T)$ are continuous functions such that $s \mapsto s\tilde{\sigma}(s, \tilde{t})$ is a Lipschitz regular function of s with a Lipschitz constant independent of $\tilde{t}$, and is bounded from above and away from 0 uniformly in $\tilde{t}$, the Black-scholes formula for an European call and put option at time $\tilde{t}$ are following (note that F_t is the filtration and $s_T(\tilde{t}) = s\,e^{\tilde{r}_{\tilde{t}}(T-\tilde{t})}$):

$$\begin{aligned} C(s, \tilde{t}) = &\quad E^*(e^{-\int_{\tilde{t}}^{T}\tilde{r}(\tau)d\tau}(s_T(\tilde{t}) - K)_+ \mid F_t) \\ P(s, \tilde{t}) = &\quad E^*(e^{-\int_{\tilde{t}}^{T}\tilde{r}(\tau)d\tau}(K - s_T(\tilde{t}))_+ \mid F_t) \end{aligned} \tag{2}$$

We can also rewrite equation (1) in the form of a partial differential equation (PDE) as follows

$$\frac{\partial P(s, \tilde{t})}{\partial \tilde{t}} + \frac{s^2\tilde{\sigma}^2(s, \tilde{t})}{2}\frac{\partial^2 P(s,\tilde{t})}{\partial s^2} + \tilde{r}(\tilde{t})\,s\frac{\partial P(s, \tilde{t})}{\partial s} - \tilde{r}(\tilde{t})\,P(s, \tilde{t}) = 0 \tag{3}$$

with the boundary conditions $P(s,\, T) = \begin{cases} K - s & \text{if } s < K \\ 0 & \text{if } s > K \end{cases}$ and $P(0,\, t) = Ke^{-r(T-t)}$.

1.2 Black-Scholes Formula

When $\tilde{\sigma}(s,\, \tilde{t}) = \sigma$ and $\tilde{r}(\tilde{t}) = r$ are constants, by using the transformation $t = T - \tilde{t}$, $x = log\, s$, and $\phi(x,\, t) = P\,(e^x,\, T - t)$, equation (**3**) becomes the Black-Scholes equation

$$\frac{\partial \phi}{\partial t} - \frac{1}{2}\sigma^2 \frac{\partial^2 \phi}{\partial x^2} - (r - \frac{\sigma^2}{2})\frac{\partial \phi}{\partial x} + r\phi = 0 \text{ as } (\mathrm{x,t}) \in \ \mathrm{R}\times[0,\mathrm{T}] \tag{4}$$

$$\phi(x,\, 0) = (K - e^x)_+ \tag{5}$$

$$\phi(x,\, t) \ \sim Ke^{-rt} \text{ as } x \to \text{-}\infty \tag{6}$$

$$\phi(x,\, t) = 0 \text{ as } \mathrm{x} \to \infty \tag{7}$$

The advantage of equation (**4**) is that it has constant coefficients, and by setting $\phi(x,\, t) = \Psi(x,\, t)\, e^{-(r + \frac{\sigma^2}{2} b^2)t + (\frac{1}{2} - \frac{r}{\sigma^2})x}$, we obtain a following one-dimensional heat equation

$$\frac{\partial \Psi}{\partial t} - \frac{\sigma^2}{2}\frac{\partial^2 \Psi}{\partial x^2} = 0 \text{ as } (x,\, t) \in \ R \times [0, T]$$

$$\Psi(x,\, 0) = (K\, e^{(\frac{-1}{2} + \frac{r}{\sigma^2})x} - e^{(\frac{1}{2} + \frac{r}{\sigma^2})x})_+$$

$$\Psi(x,\, t) = 0 \text{ as } \mathrm{x} \to \infty$$

Solving the heat equation above with the given boundary conditions, we obtain the explicit Black-Scholes formula for the price of vanilla European put (or call option by using the same transformation but with some modifications to the boundary conditions (**5**) – (**7**))

$$\begin{aligned} C(s,\tilde{t}) = &\quad s\,N(d_1) - Ke^{-r(T-\tilde{t})}N(d_2) \\ P(s,\tilde{t}) = &\quad -s\,N(-d_1) + Ke^{-r(T-\tilde{t})}N(-d_2) \end{aligned} \tag{8}$$

where $N(d) = \frac{1}{\sqrt{2\pi}}\int_{-\infty}^{d} e^{\frac{-y^2}{2}}dy$, K is the exercise price or strike price of a call or put option, $d_1 = \frac{log(\frac{s}{K})+(r+\frac{\sigma^2}{2})(T-\tilde{t})}{\sigma\sqrt{T-\tilde{t}}}$ and $d_2 = d_1 - \sigma\sqrt{T-\tilde{t}}$.

Remark 1.2. If $\tilde{r}(\tilde{t})$ is not a constant, $d_1 = \frac{log(\frac{s}{K})+\int_{\tilde{t}}^{T}\tilde{r}(\tau)d\tau+(\tilde{r}+\frac{\sigma^2}{2})(T-\tilde{t})}{\sigma\sqrt{T-\tilde{t}}}$ and d_2 is the same as above

1.3 Constant Elasticity of Variance (CEV) Model

Although pricing derivatives under the assumption of constant volatility, as in the Black-Scholes model (equation (3) with constant σ and r) for an European put option pricing, is well-known to give results which cannot be reconciled with market observations, such problem did not widely manifest themselves until the 1987 market crash. After this event, many stochastic volatility models, such as Heston model, Stochastic Alpha-Beta- Rho model, were introduced as ideal approaches to resolve a shortcoming of the Black-Scholes model. In particular, since the Black-Scholes model assumes that the underlying volatility is constant over the life of the derivative, and unaffected by changes in the price level of the underlying security, such model cannot explain long-observed features of the volatility smile and skew, which indicate that implied, or local, volatility does tend to vary with respect to the strike price and expiry time. By assuming that the volatility of the underlying price is a stochastic process rather than a constant, it becomes possible to model prices of the derivatives more accurately.

One of the most popular stochastic volatility models, which is widely used in practice, is the Constant Elasticity of Variance (CEV) model. It was first proposed by Cox & Ross (see [4]) as an alternative to the Black-Scholes model of underlying asset price movements. The CEV model describes the following relationship between the volatility and price,

$$ds = \mu s\,d\tilde{t} + \sigma_0 s^{\gamma} dW_{\tilde{t}}$$

where σ_0, γ are constant parameters satisfying $\sigma_0 \geq 0$ and $\gamma > -1$, $W_{\tilde{t}}$ is a standard Brownian motion, s is the price of an underlying asset at time $\tilde{t}$ and μ is the expected return. The term $\sigma_0 s^{\gamma}$ denotes an instantaneous, or local, volatility of our option. We use the Finite Element method introduced in

Section (2) to solve numerically the following PDE, given the two boundary conditions, of an European put option whose local volatility is $\tilde{\sigma}(s,\, t) = \sigma_0 s^{\gamma}$,

$$\frac{\partial u(s,\, t)}{\partial t} - \frac{\sigma_0^2 s^{2+2\gamma}}{2}\frac{\partial^2 u\,(s,\, t)}{\partial s^2} - rs\frac{\partial u\,(s,\, t)}{\partial s} + ru\,(s,\, t) = 0 \tag{9}$$

$$u\,(0,\, t) = Ke^{-rt} \tag{10}$$

$$u(s,\, 0) = \begin{cases} K - s & \text{if } s < K \\ 0 & \text{if } s > K \end{cases} \tag{11}$$

1.4 Remarks about the Black-Scholes equation

On the other hand, when $\tilde{\sigma}(s,\, \tilde{t})$ and $\tilde{r}(\tilde{t})$ are not constants, since $t = T - \tilde{t}$, we let $u(s,\, t) = P(s,\, T - t)$, $\sigma(s,\, t) = \tilde{\sigma}(s,\, T - t)$ and $r(t) = \tilde{r}(T - t)$. Assume that for each time t, define $q(t) = \tilde{q}(T - t)$ as the dividend yield, and the underlying asset pays out a dividend $q(t)s\,dt$ in dt, equation (3) becomes (note that $s > 0$ and $t \in [0,\, T]$)

$$\frac{\partial u(s,\, t)}{\partial t} - \frac{\sigma^2(s,\, t)\, s^2}{2}\frac{\partial^2 u(s,\, t)}{\partial s^2} - (r(t) - q(t))s\,\frac{\partial u(s,\, t)}{\partial s}$$

$$+r(t)\, u(s,\, t) = 0 \tag{12}$$

with the Cauchy data $u(s,\, 0) = u^0(s)$ where $s \in R_+$ and u^0 is the payoff function.

If q is sufficently well-behaved, then equation (**12**) does not have any additional mathematical difficulties compared to equation (3). Thus, we assume that $q(t) = 0$, which implies there are no discretely paid dividends. This means the equation of an American vanilla call option is exactly the same as that of an European one, which is equation (**3**).
The Cauchy problem (**12**) can then be proved, with additional conditions:

- The function $(s,\, t) \longmapsto s\sigma(s,\, t)$ is Holder regular on $R_+ \times [0,\, T]$.

- The function $\sigma(s,\, t)$ is bounded on $R_+ \times [0,\, T]$ and bounded below by a positive constant.
- The function $t \mapsto r(t)$ is bounded and Lipschitz continuous.
- The Cauchy data P_0 satisfies $0 \leq u_0(s) \leq C(1+s)$ for a given constant$C$.

then there exists an unique function $u \in C^0(R_+ \times [0,\, T])$, C^1-regular with respect to t and C^2-regular with respect to s, which is solution to the boundary-value problem (**12**) and satisfies $0 \leq u(s,\, t) \leq C'(1+s)$ for a given constant C'.

1.5 Variational Formulation

Since our underlying asset does not pay any dividends, by letting $g(s,\, t) = C(s,\, T-t)$, we introduce the well-known put-call parity as follows

$$g\,(s,\, t) - u\,(s,\, t) = s - Ke^{-rt} \tag{13}$$

We would like to solve the following equation to determine the approximated price of an European vanilla put option with one underlying asset for which the annual interest rate $r(t) = r$ is constant and the local volatility $\sigma(s,\, t)$ is variable, with the boundary conditions derived from the put-call parity, equation (**13**), given the time to maturity $t = 1$, and $g\,(0,\, t) = 0$ when $s = 0$.

$$\frac{\partial u(s,\, t)}{\partial t} - \frac{\sigma^2\,(s,\, t)\, s^2}{2}\frac{\partial^2 u\,(s,\, t)}{\partial s^2} - rs\frac{\partial u\,(s,\, t)}{\partial s} + ru\,(s,\, t) = 0 \tag{14}$$

$$u\,(0,\, t) = Ke^{-rt} \tag{15}$$

$$u(s,\, 0) = \begin{cases} K - s & \text{if } s < K \\ 0 & \text{if } s > K \end{cases} \tag{16}$$

By defining the space $V = \{v \in L^2(R_+) : v\frac{dv}{ds} \in L^2(R_+)\}$,
$C^0([0,1];\, L^2(R_+))$ as the space of continuous function on$[0,1]$ with values in $L^2(R_+)$, and $L^2(0,1;V)$ as the space of square integrable functions on$(0,1)$ with values in V, we can write the **variational formulation** of the Boundary-Value Problem$(\mathbf{14}) - (\mathbf{16})$ as follows

Weak Variational Problem. Find $u \in C^0([0,1];\, L^2(R_+)) \cap L^2(0,1;V)$ such that $\frac{\partial u}{\partial t} \in L^2(0,1;\, V')$, where V' is a topological dual space of V, satisfying

$$\forall v \in V, \qquad a_t(u,\, v) + \int_{R_+} v\frac{\partial u}{\partial t} ds = 0 \tag{17}$$

$$u\,(0,\, t) = Ke^{-rt}$$

$$u(s,\, 0) = \begin{cases} K - s & \text{if } s < K \\ 0 & \text{if } s > K \end{cases}$$

where $a_t(u,\, v)$ is called the bilinear form,

$$a_t(u,\, v) = \textstyle\int_{R_+} \frac{\sigma^2(s,t)s^2}{2} \frac{\partial u}{\partial s}\frac{\partial v}{\partial s} ds$$

$$+r \textstyle\int_{R_+} uv\, ds$$

$$+ \textstyle\int_{R_+} \left(-r + \sigma^2\,(s,\, t) + s\sigma\,(s,\, t)\, \frac{\partial \sigma}{\partial s}\,(s,\, t)\right) s\frac{\partial u}{\partial s} v\, ds$$

We now introduce the Finite Element Method (FEM) and apply this method using Ritz-Galerkin approach, together with Crank-Nicolson implicit scheme for different discretizations in the S-T directions (i.e, different S-T-lattices) to find the approximated prices of an European put option with constant or variable local volatility. Such problem is equivalent to find the numerical solution to the weak variational problem (equation $(\mathbf{17})$). We then compare our numerical solutions to the exact solutions

given by the classic Black-scholes formula to measure the errors of our numerical scheme in L^2- norm and L^∞- norm. We compare the errors to see which mesh refinement gives the most accurate numerical solutions (that is, the closest one to the exact solution). Finally, for an European put option with variable local volatility in which the Black-Scholes formula is not a reliable tool, we use FEM combining with the most efficient mesh refinements determined from previous experiments to obtain the approximated prices for each time t and to understand the behavior of the solution when we consider different values of σ.

2 The Finite Element Method

Compared to the Finite Differences Method (FDM) whose lattice is basically rectangular and adaption to non-trivial geometric domain is difficult, the FEM is far more flexible due to the following typical properties:

- Division of the domain into simple geometric subdomains, such as rectangles (for 1D domain), triangles and/or quadrilaterals (for 2D domain), or cubes (for 3D domain)
- Setup of test-functions (continuous piecewise polynomials) on subdomains
- Global assembling of test functions

FEM can be applied to the variational formulation of a PDE, such as equation (**17**), or the variational inequality, which is often derived from the free-boundary conditions of American option.

2.1 Subdivision of the Domain

Let $\Omega \subset \mathbb{R}$ denote the domain. We want to find a partition P of Ω, which consists of dividing the two intervals in S and T directions,$[0,\ S_b]$ and $[0,\ T]$, into N_s and N_t subintervals $\Gamma_i = [s_{i-1},\ s_i]$ and $T_k = [t_{k-1},\ t_k]$ such that $h_i = s_i - s_{i-1}$ and $\triangle t_k = t_k - t_{k-1}$, respectively ($i = 1, 2, ..., N_s$ and $k = 1, 2, ..., N_t$). We can either use an equidistant or nonequidistant partition for the S and T direction. Figure 1 gives an example for a $S-T$-lattice with uniform partitions in both S and T directions.

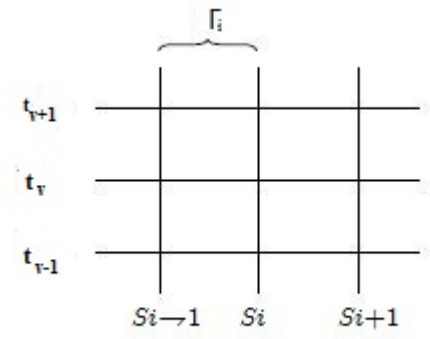

Figure 1: Partition of Ω into rectangle $S-T$-lattice

We introduce the following definition for an uniform and geometric parition on the interval $[0,\ S_b]$, also defined as the S-direction.

- Partition of the interval $[0,\ S_b]$ into subintervals $\Gamma_i = [s_{i-1},\ s_i]$, $1 \leq i \leq N_s$ such that $0 = s_0 < s_1 < \cdots < s_{N_s} = S_b$ and $h_1 = h_2 = ... = h_{N_s}$. Let $\Gamma_q = max_{i=1,...,N_s}\Gamma_i$, and the mesh Γ of $[0,\ S_b]$ be the set $\{\Gamma_1, \Gamma_2, ..., \Gamma_{N_s}\}$. Realistically, we will assume that the strike price K of our put option coincides with some nodes of Γ, which means there exists z such that $s_z = K$. This partition is defined as the "uniform partition" in the s-direction.

- Partition of the interval $[0,\, S_b]$ into two intervals $[0,\, K]$ and $[K,\, S_b]$. Each of these intervals is partitioned as follows: we divide the intervals $[0,\, K]$ and $[K,\, S_b]$ into N_1 and N_2 subintervals, $\Gamma_i = [s_{i-1},\, s_i]$ and $\Gamma_j = [s_{j-1},\, s_j]$ $(1 \leq i \leq N_1,\ N_1 + 1 \leq j \leq N_1 + N_2)$, such that $0 = s_0 < s_1 < \cdots < s_{N_1} = K < \cdots < s_{N_2} = S_b$, $h_{N_1} = r_1^{N_1-1} h_1 = h_1^{\frac{4}{3}}$ and $h_{N_1+1} = r_2^{N_2-1} h_{N_1+N_2} = h_{N_1+N_2}^{\frac{4}{3}}$ for $0 \leq r_1,\, r_2 \leq 1$ (the reason for the choice $h_1^{\frac{4}{3}}$ and $h_{N_1+N_2}^{\frac{4}{3}}$ is because when taking a small step in the S-direction, and plotting the L_2-norm errors with respect to different number of timesteps in the T-direction, the convergence order is less than 2, and in fact, the errors decay slower than $h_1^{\frac{3}{4}}$ and $h_{N_1+N_2}^{\frac{3}{4}}$) for $0 \leq r_1,\, r_2 \leq 1$.

We now show that if h_1 is given, the values of r_1 and N_1 are uniquely determined (same arguments for finding r_2 and N_2 in the interval $[K,\, S_b]$). Notice that since $h_{i=1,2,\ldots,N_1}$ follows a geometric series in the interval $[0,\, K]$, $h_1 + h_1 r_1 + \ldots + h_1 {r_1}^{N_1-1} = \frac{h_1(1-r_1^{N_1})}{1-r_1} = K$. Since $r_1^{N_1-1} h_1 = h_1^{\frac{4}{3}}$, we obtain $\frac{h_1 - h_1^{\frac{4}{3}} r_1}{1-r_1} = K$. Solving for r_1, we get $r_1 = \frac{K-h_1}{K-h_1^{\frac{4}{3}}}$. Furthermore, since $r_1^{N_1-1} = h_1^{\frac{1}{3}}$, solving for N_1 gives $N_1 = \frac{1}{3}\frac{log\, h_1}{log\, r_1} + 1$. Therefore, given the value of h_1, there exists an unique pair

$$(r_1,\, N_1) = (\frac{K-h_1}{K-h_1^{\frac{4}{3}}},\, \frac{1}{3}\frac{log\, h_1}{log\, r_1} + 1)$$

satisfying all the given restriction. Similarly, an unique pair

$$(r_2,\, N_2) = (\frac{S_b - K - h_{N_1+N_2}}{S_b - K - h_{N_1+N_2}^{\frac{4}{3}}},\, \frac{1}{3}\frac{log\, h_{N_1+N_2}}{log\, r_2} + 1)$$

exists for the interval $[K,\, S_b]$.

Finally, let $\Gamma_q = max_{i=1,\ldots,N_1+N_2}\Gamma_i$, and the mesh Γ of $[0,\, S_b]$ as the set $\{\Gamma_1, \Gamma_2, ..., \Gamma_{N_1+N_2}\}$. Realistically, we will assume that the strike price K of our put option coincides with some nodes of Γ, which means there exists N_1 such that $s_{N_1} = K$. This partition is defined as a "geometric partition" in the s-direction. Our main purpose for discretizing the s-direction in this way is to increase significantly the number of points s_i near K where the singularity occurs, so that the accuracy of our numerical solutions is increased.

For the accuracy conditions of our numerical schemes, the similar partitions are used for the interval $[0,\, T]$. Specifically, we will choose $(\triangle t_1)^{\frac{8}{3}}$ for the same reasons used to choose $h_1^{\frac{4}{3}}$.

2.2 The Ritz - Galerkin Approach

For numerical computation, Ritz and Galerkin suggested to treat the variational problem on a finitely-dimensional Hilbert subspace $V_h^b \subseteq H_0^1$(the Hilbert space of functions with square-integrable value and derivatives in Ω with zero value on the boundary $\partial\Omega$). V_h^b is called trial space. Therefore, we consider the discrete variational problem to find $u_h \in V_h^b$, which is the solution of

$$a\left(u_h(s),\, v_h(s)\right) = \int_\Omega f(s)v_h(s)ds \quad \text{for all } v_h \in V_h^b \tag{18}$$

where $\int_\Omega f(s)v_h(s)ds = (f,\, v_h)$ and $a\left(u_h(s),\, v_h(s)\right)$ is a bilinear form stated in the weak variational problem. Let $\varphi_1, \varphi_2, ..., \varphi_k$ be a basis of V_h^b, with $k = dim\left(V_h^b\right)$. Then the u_h in (**18**) can be interpolated by the basis elements with corresponding weights $\varphi_j \in R$ in the following way:

$$u_h = \sum_{j=1}^{k} u_{h,\,j}\varphi_j \tag{19}$$

By means of the Finite Element method, the φ_j are call basis or test functions, which we will use later on as piecewise well-definied polynomials. The representation of u_h as a finite sum of weighted test functions, in fact, gives the name "Finite Element Method." Using (**19**), we can rewrite the discrete variational problem (**18**) as:

Find a $u_h \in V_h^b$ with

$$\begin{aligned} a(u_h,\, v_h) &= (f,\, v_h)\ \forall\, v_h \in V_h^b \iff \\ a(u_h,\, \varphi_i) &= (f,\, \varphi_i)\ \forall\, i = 1, ..., k \iff \end{aligned}$$

$$\begin{aligned} a(\textstyle\sum_{j=1}^{k} u_{h,\,j}\varphi_j\varphi_i) &= (f,\, \varphi_i)\ \forall\ i = 1, ..., k \iff \\ \textstyle\sum_{j=1}^{k} a(\varphi_j,\, \varphi_i)u_{h,\,j} &= (f,\, \varphi_i)\ \forall\ i = 1, ..., k \iff \end{aligned}$$

$$Au_h = B \tag{20}$$

with $A := (a(\varphi_j, \varphi_i))_{i,,j} \in R^{k\times k}$, $u_h := (u_{h,1}, ..., u_{h,k}))^T$ and
$B := (f, \varphi_i)_i$, $i = 1, ..., k$.

Hence, the Ritz-Galerkin approach is equivalent to a linear system of equations, and the computation of vector u_h, applied to equation (**20**), gives an approximation for u. Due to its application to mechanics, A is called the stiffness matrix. It is positive definite and symmetric for an arbitrary basis $\varphi_1, ..., \varphi_k$, which implies A is invertible. Note that for certain choices of the basis, the matrix A is sparse, which means that only a few elements $(A)_{i,j}$ are non-zero. This would reduce the cost for the computation of (20) significantly.

2.3 Finite Element Method applied to European Vanilla Option

We now define the discrete space V_h^b as follows to ensure that the boundary condition $u(s, 0) = 0$ for $s > K$ belongs to V_h^b,

$$V_h^b = \left\{\varphi(s) \in C^0[0, S_b], \varphi(S_b) = 0 \ \forall s \in \Gamma, \varphi_{|s} \text{ is affine}\right\}$$

In the real world, the option value is dependent mainly on the underlying asset price s whose local volatility varies based on the changes in the values of s. Therefore, we consider the general case when the local volatility σ, which is a function of s and t, is described through the CEV model $\sigma(s, t) = \sigma_0 s^\gamma$ for constant parameters $\sigma_0 \geq 0$, $\gamma > -1$ and s is the price of an underlying asset at time t. We rewrite equation (**14**) in the following form where $\alpha = \frac{s^{2(1+\gamma)}\sigma_0^2}{2}$, $\beta = (1+\gamma)\sigma_0^2 s^{2\gamma+1} - rs$,

$$\frac{\partial u}{\partial t} - \frac{\partial}{\partial s}(\alpha\frac{\partial u}{\partial s}) + \beta\frac{\partial u}{\partial s} + ru = 0 \tag{21}$$

Multiplying both sides by the test function $\varphi(s) \in V_h^b$, and by using integration by parts for the term $\int_0^{S_b} \varphi(s)\frac{\partial}{\partial s}(\alpha\frac{\partial u}{\partial s})\,ds = -\int_0^{S_b} \alpha\frac{\partial u}{\partial s}\frac{\partial \varphi(s)}{\partial s}ds$ (since $\varphi(S_b) = 0$) , equation (**21**) becomes

$$(\frac{\partial u}{\partial t},\, \varphi) + (\alpha\frac{\partial u}{\partial s},\, \frac{\partial \varphi}{\partial s}) + (\beta\frac{\partial u}{\partial s},\, \varphi) + (ru,\, \varphi) \,= 0 \tag{22}$$

where $(\cdot, \cdot)$ is a broken L^2 inner product with respect to all partitions Γ_i of the interval $[0,\, S_b]$.

Let u_t denote $\frac{\partial u}{\partial t}$, and u_h^k denote $u_h(\cdot,\, t_k)$. After discretizing equation (**22**) in space and time (dividing the interval $[0, 1]$ into N_t subintervals $[t_k,\, t_{k-1}]$, $k = 1, \ldots, N_t$ with lengths $\triangle t_k = t_k - t_{k-1}$) and rewriting $u_h(s,\, t_k) = \sum_{i=1}^{2} u_{h,\,i}(t_k)\varphi_i(s)$, where φ_i is the nodal basis of V_h^b, we obtain the fully discrete variational problem with two boundary conditions:
Find $u_h(s,\, t_k) \in V_h^b$ such that

$$u_h^0 = max(K - s,\, 0) \;\text{ for } s \text{ is the price of the underlying asset}$$

$$\text{at time } t \,= 0 \tag{23}$$

$$u_h(0,\, t_k) \,= Ke^{-rt_k} \tag{24}$$

and for $1 \leq k \leq N_t$,

$$M(u_h(s,\, t_k),\, \varphi) + A(u_h(s,\, t_k),\, \varphi) = 0 \;\; \forall\, \varphi \in V_h^b \text{ and } \;\; t_k \in [0,\, 1] \tag{25}$$

where $m\left(u_h^k,\, \varphi\right)$ is the inertial form of the mass matrix M,

$$m(u_h(s,\, t_k),\, \varphi) \,= (u_h(s,\, t_k),\, \varphi) \tag{26}$$

and $a(u_h^k,\, \varphi)$ is the Galerkin form of the stiffness matrix A,

$$a(u_h(s,\, t_k),\, \varphi) \;\; = \;\; (\alpha\frac{\partial u_h^k}{\partial s},\, \frac{\partial \varphi}{\partial s}) + (\beta\frac{\partial u_h^k}{\partial s},\, \varphi) + (ru_h^k,\, \varphi) \tag{27}$$

Let $(\alpha\frac{\partial u_h^k}{\partial s},\, \frac{\partial \varphi}{\partial s}) \,= a^{1,\,k}$, $(\beta\frac{\partial u_h^k}{\partial s},\, \varphi) \,= a^{2,\,k}$, $(ru_h^k,\, \varphi) \,= a^{3,\,k}$, the equation (**27**) can be rewritten as follows

$$a(u_h(s,\, t_k),\, \varphi) \,= a^{1,\,k} + a^{2,\,k} + a^{3,\,k} \tag{28}$$

Given $u_h^0 \,= max(K - s,\, 0)$, we can use either the Euler explicit/implicit scheme or the second-order stable Crank-Nicolson scheme corresponding to the values of $\theta = 0,\, \frac{1}{2},\, 1$, respectively, to find u_h^k for $k = 1, 2, \ldots, N_t$ from the equation

$$\frac{1}{\triangle t_k} m(u_h^k - u_h^{k-1},\, \varphi) \,+\, a(\theta u_h^k + (1-\theta) u_h^{k-1},\, \varphi) \,= 0 \;\forall\; \varphi \in V_h^b \tag{29}$$

In order to obtain the most accurate and stable numerical solutions for large local volatility, we choose the second-order stable Crank-Nicolson scheme (that is, $\theta = \frac{1}{2}$). Now, for each finite element defined over the nodes $(s_i,\, s_j)$, the mass matrix M has its entries $m_{i,\,j} \,= (\varphi_j,\, \varphi_i)$, and let A be the stiffness matrix defined by

$$a_{i,\,,j} = a\left(\varphi_j,\, \varphi_i\right) = a^1_{i,\,j} + a^2_{i,\,j} + a^3_{i,\,j},\; 0 \,\leq i,\, j \,\leq N_s$$

By letting $u_h^k \;=\; \left(u_h^k\left(s_0\right), ..., u_h^k\left(s_N\right)\right)^T$ and $u_h^0 \;=\; \left(u_h^0\left(s_0\right), ..., u_h^0\left(s_N\right)\right)^T$, which is the boundary condition, we can rewrite equation (**29**) as follows

$$M\left(u_h^k - u_h^{k-1}\right) + \frac{\triangle t_k}{2}\left(A u_h^k + A u_h^{k-1}\right) = 0$$

$$\Longleftrightarrow (M + \frac{\triangle t_k}{2} A) u_h^k = (M - \frac{\triangle t_k}{2} A) u_h^{k-1}$$

We now choose the nodal basis φ_i to be the hat functions, which were defined below over two consecutive nodes s_i,s_{i-1} and $s_i,\, s_{i+1}$.

Definition 1.2 (Hat Functions) With $i \,= 0, 1, \ldots, N_s$, the hat functions are

$$\varphi_i\left(s\right) = \frac{s - s_{i-1}}{h_i} \;\forall\, s \in (s_{i-1},\, s_i)$$

$$\varphi_i\left(s\right) \;\; = \frac{s_{i+1} - s}{h_{i+1}} \;\forall\, s \;\in (s_i,\, s_{i+1})$$

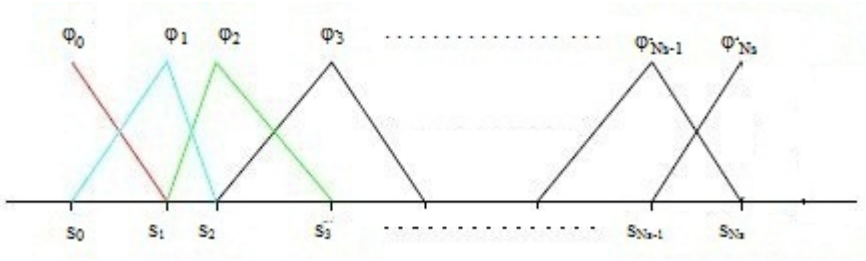

Figure 2: Setup of the hat functions

Note that the first and last element φ_0 and φ_{N_s} need to be cut off to fit into the discretized domain, as shown in Figure 2. These hat functions φ_i correspond to the nodes s_i and are supported in $[s_{i-1},\, s_{i+1}]$. When $|i-j|> 1$, the intersection of the support φ_i and φ_j has measure 0. This implies the matrices M and A are tridiagonal. We now compute the actual assembling of matrix M as follows: by definition, $m_{i,,j} = (\varphi_j,\, \varphi_i)_{i,\, j=0,\ldots,\, N_s}$ with $(\varphi_j,\, \varphi_i) = \int_0^{S_b} \varphi_i \varphi_j \, ds$.

The first element of M, $m_{0,0}$ and $m_{N_s,\, N_s}$ just contains one of the two summands of the equation (**34**), since it is defined by the cut boundary finite element φ_0 and φ_{N_s}. The calculations for $m_{0,0}$ and $m_{N_s,\, N_s}$ are follows,

$$\begin{aligned} m_{0,0} = \int_0^{S_b} \varphi_0 \varphi_0 ds = \int_{s_0}^{s_1} (\varphi_0)^2 ds \; &= \int_{s_0}^{s_1} \frac{1}{h_1^2} (s_1 - s)^2 \, ds \\ &= -\frac{1}{3h_1^2} (-s_1 + s_0)^3 = \frac{h_1}{3} \end{aligned} \tag{30}$$

$$\begin{aligned} m_{N_s,\, N_s} = \int_0^{S_b} \varphi_{N_s} \varphi_{N_s} ds &= \int_{s_{N_s-1}}^{s_{N_s}} (\varphi_{N_s})^2 ds \\ &= \int_{s_{N_s-1}}^{s_{N_s}} \frac{1}{h_{N_s}^2} (s_{N_s} - s_{N_s-1})^2 \, ds \\ &= -\frac{1}{3h_{N_s}^2} (-s_{N_s} + s_{N_s-1})^3 = \frac{h_{N_s}}{3} \end{aligned} \tag{31}$$

The matrix M is symmetric, since both subdiagonals $m_{i,\,i-1}$ and $m_{i,\,i+1}$ have the following formulas for its entries

$$m_{i,\,i+1} = \int_0^{S_b} \varphi_{i+1}\varphi_i \, ds \; = \int_{s_i}^{s_{i+1}} \frac{1}{h_{i+1}^2} \left(s - s_i\right)\left(s_{i+1} - s\right) ds$$

$$= \frac{1}{h_{i+1}^2}\left(\frac{s_{i+1}s^2}{2} - s_{i+1}s_i s - \frac{s^3}{3} + \frac{s_i s^2}{2}\right)\Big|_{s_i}^{s_{i+1}}$$

$$= \frac{1}{h_{i+1}^2}\left(\frac{s_{i+1}^3}{6} - \frac{s_{i+1}^2 s_i}{2} + \frac{s_{i+1}s_i^2}{2} - \frac{s_i^3}{6}\right)$$

$$= \frac{1}{6h_{i+1}^2}(s_{i+1} - s_i)^3 = \frac{h_{i+1}}{6} \quad \text{for } i = 0, \ldots, N_s - 1 \tag{32}$$

$$m_{i,\,i-1} = \int_0^{S_b} \varphi_{i-1}\varphi_i ds \; = \int_{s_{i-1}}^{s_i} \frac{1}{h_i^2} \left(s - s_{i-1}\right)\left(s_i - s\right) ds$$

$$= \frac{1}{h_i^2}\left(\frac{s_i s^2}{2} - s_{i-1}s_i s - \frac{s^3}{3} + \frac{s_{i-1}s^2}{2}\right)\Big|_{s_{i-1}}^{s_i}$$

$$= \frac{1}{h_i^2}\left(\frac{s_i^3}{6} - \frac{s_i^2 s_{i-1}}{2} + \frac{s_i s_{i-1}^2}{2} - \frac{s_{i-1}^3}{6}\right)$$

$$= \frac{1}{6h_i^2}(s_i - s_{i-1})^3 = \frac{h_i}{6} \quad \text{for } i = 1, \ldots, N_s \tag{33}$$

On the diagonal of M, the elements $m_{i,\,i}$ are

$$m_{i,\,i} = \int_0^{S_b} \varphi_i\varphi_i \, ds \; = \int_{s_{i-1}}^{s_i} \left(\frac{1}{h_i}\left(s - s_{i-1}\right)\right)^2 ds$$

$$+ \int_{s_i}^{s_{i+1}} \left(\frac{1}{h_{i+1}}\left(s_{i+1} - s\right)\right)^2 ds$$

$$= \frac{1}{3h_i^2}(s_i - s_{i-1})^3 - \frac{1}{3h_{i+1}^2}(-(s_{i+1} - s_i)^3)$$

$$= \frac{h_i + h_{i+1}}{3} = 2(m^1_{i+1} + m^1_{i-1}) \quad \text{for } i = 1, \ldots, N_s - 1 \tag{34}$$

Now, for assembling matrix A, we need to compute the sum $a^1_{i,\,j} + a^2_{i,\,j} + a^3_{i,\,j}$ for $j \in \{0,\, i-1,\, i,\, i+1,\, N_s\}$. For example, similar to $m_{0,\,0}$ and $m_{N_s,\,N_s}$, $a_{0,\,0}$ and $a_{N_s,\,N_s}$ needs special treatment and requires the following computations

$$a^1_{0,\,0} = \frac{\sigma_0^2}{2} \int_0^{S_b} s^{2(1+\gamma)} (\frac{\partial \varphi_0}{\partial s})^2 \, ds \; = \frac{\sigma_0^2}{2} \int_0^{s_1} \frac{s^{2(1+\gamma)}}{h_1^2} \, ds$$

$$= \frac{\sigma_0^2 s_1^{1+2\gamma}}{2(3+2\gamma)} \tag{35}$$

$$a^2_{0,\,0} \quad = (1+\gamma)\sigma_0^2 \int_0^{S_b} s^{2\gamma+1} \varphi_0 \frac{\partial \varphi_0}{\partial s} ds - r \int_0^{S_b} s \varphi_0 \frac{\partial \varphi_0}{\partial s}$$

$$= -\frac{(1+\gamma)\sigma_0^2}{h_1^2} (\frac{s_1^{3+2\gamma}}{2+2\gamma} - \frac{s_1^{3+2\gamma}}{3+2\gamma}) + \frac{r s_1^3}{6h_1^2}$$

$$= -\frac{\sigma_0^2 s_1^{1+2\gamma}}{2(3+2\gamma)} + \frac{r s_1}{6} \text{ , since } s_0 = 0 \text{ and } h_1 = s_1 \tag{36}$$

$$a^3_{0,\,0} = r \int_0^{S_b} (\varphi_0)^2 \, ds \; = r \int_0^{s_1} \frac{(s_1 - s)^2}{h_1^2} \, ds = \frac{r h_1}{3} \tag{37}$$

$$a^1_{N_s,\,N_s} = \frac{\sigma_0^2}{2} \int_0^{S_b} s^{2(1+\gamma)} (\frac{\partial \varphi_{N_s}}{\partial s})^2 \, ds$$

$$= \frac{\sigma_0^2}{2} \int_{s_{N_s-1}}^{s_{N_s}} \frac{s^{2(1+\gamma)}}{h_{N_s}^2} \, ds$$

$$= \frac{\sigma_0^2}{2h_{N_s}^2} (\frac{s_{N_s}^{3+2\gamma} - s_{N_s-1}^{3+2\gamma}}{3+2\gamma})$$

$$a^2_{N_s,\,N_s} = (1+\gamma)\sigma_0^2 \int_0^{S_b} s^{2\gamma+1} \varphi_{N_s} \frac{\partial \varphi_{N_s}}{\partial s} ds$$

$$-r \int_0^{S_b} s \varphi_{N_s} \frac{\partial \varphi_{N_s}}{\partial s}$$

$$= \frac{(1+\gamma)\sigma_0^2}{h_{N_s}^2}\left(\frac{s_{N_s}^{2\gamma+3}}{2\gamma+3} - \frac{s_{N_s}^{2\gamma+2}s_{N_s-1}}{2\gamma+2}\right)$$

$$+\frac{\sigma_0^2 s_{N_s-1}^{2\gamma+3}}{2h_{N_s}^2(2\gamma+3)} - \frac{r}{h_{N_s}^2}\left(\frac{s_{N_s}^3}{3} + \frac{s_{N_s-1}^3}{6}\right)$$

$$+\frac{r s_{N_s}^2 s_{N_s-1}}{2h_{N_s}^2}$$

$$= \frac{(1+\gamma)\sigma_0^2}{h_{N_s}^2}\left(\frac{s_{N_s}^{2\gamma+3}}{2\gamma+3}\right) - \frac{\sigma_0^2 s_{N_s}^{2\gamma+2}s_{N_s-1}}{2h_{N_s}^2}$$

$$+\frac{\sigma_0^2}{h_{N_s}^2}\frac{s_{N_s-1}^{2\gamma+3}}{2(2\gamma+3)} - \frac{r\left(2s_{N_s}+s_{N_s-1}\right)}{6} \tag{38}$$

$$a_{N_s,N_s}^3 = r\int_0^{S_b}(\varphi_{N_s})^2\,ds = r\int_{S_{N_s-1}}^{s_{N_s}}\frac{(s-s_{N_s-1})^2}{h_{N_s}^2}\,ds$$

$$= \frac{rh_{N_s}}{3} \tag{39}$$

For the elements $a_{i,i-1}$, we need to calculate the following elements

$$a_{i,i-1}^1 = \frac{\sigma_0^2}{2}\int_0^{S_b} s^{2(\gamma+1)}\frac{\partial\varphi_i}{\partial s}\frac{\partial\varphi_{i-1}}{\partial s}\,ds$$

$$= -\frac{\sigma_0^2}{2}\int_{s_{i-1}}^{s_i}\frac{s^{2(\gamma+1)}}{h_i^2}\,ds$$

$$= -\frac{\sigma^2}{2h_i^2}\left(\frac{s_i^{2\gamma+3}-s_{i-1}^{2\gamma+3}}{2\gamma+3}\right) \tag{40}$$

$$a_{i,i-1}^2 = (1+\gamma)\sigma_0^2\int_0^{S_b} s^{2\gamma+1}\varphi_i\frac{\partial\varphi_{i-1}}{\partial s}\,ds - r\int_0^{S_b} s\varphi_i\frac{\partial\varphi_{i-1}}{\partial s}\,ds$$

$$= -\frac{(1+\gamma)\sigma_0^2}{h_i^2}\left(\frac{s_i^{2\gamma+3}}{2\gamma+3} - \frac{s_i^{2\gamma+2}s_{i-1}}{2\gamma+2}\right)$$

$$+\frac{r}{h_i^2}\left(\frac{s_i^3}{3} - \frac{s_i^2 s_{i-1}}{2} + \frac{s_{i-1}^3}{6}\right)$$

$$- \frac{\sigma_0^2 s_{i-1}^{2\gamma+3}}{2h_i^2(2\gamma+3)}$$

$$= \frac{-(1+\gamma)\sigma_0^2}{h_i^2}\frac{s_i^{2\gamma+3}}{2\gamma+3} - \frac{\sigma_0^2 s_i^{2\gamma+2}s_{i-1}}{2h_i^2}$$

$$- \frac{\sigma_0^2}{h_i^2}\frac{s_{i-1}^{2\gamma+3}}{2(2\gamma+3)} + \frac{r(2s_i+s_{i-1})}{6} \tag{41}$$

$$a_{i,\,i-1}^3 = rm_{i,\,i-1}^1 = r\frac{h_i}{6} \tag{42}$$

For the elements $a_{i,\,i+1}$, we need to calculate the elements

$$a_{i,\,i+1}^1 = \frac{\sigma_0^2}{2}\int_0^{S_b} s^{2\gamma+2}\frac{\partial\varphi_i}{\partial s}\frac{\partial\varphi_{i+1}}{\partial s}\,ds$$

$$= -\frac{\sigma_0^2}{2}\int_{s_i}^{s_{i+1}} \frac{s^{2\gamma+2}}{h_{i+1}^2}\,ds$$

$$= -\frac{\sigma^2}{2h_{i+1}^2}(\frac{s_{i+1}^{2\gamma+3}-s_i^{2\gamma+3}}{2\gamma+3}) \tag{43}$$

$$a_{i,\,i+1}^2 = (1+\gamma)\sigma_0^2\int_0^{S_b} s\varphi_i\frac{\partial\varphi_{i+1}}{\partial s}\,ds - r\int_0^{S_b} s\varphi_{i+1}\frac{\partial\varphi_i}{\partial s}\,ds$$

$$= \frac{(1+\gamma)\sigma_0^2}{h_{i+1}^2}(-\frac{s_i^{2\gamma+2}s_{i+1}}{2\gamma+2} + \frac{s_i^{2\gamma+3}}{2\gamma+3})$$

$$- \frac{r}{h_{i+1}^2}(\frac{s_{i+1}^3}{6} - \frac{s_i^2 s_{i+1}}{2} + \frac{s_i^3}{3})$$

$$+ \frac{\sigma_0^2}{h_{i+1}^2}\frac{s_{i+1}^{2\gamma+3}}{2(2\gamma+3)}$$

$$= \frac{(1+\gamma)\sigma_0^2}{h_{i+1}^2}\frac{s_i^{2\gamma+3}}{2\gamma+3} - \frac{\sigma_0^2 s_i^{2\gamma+2}s_{i+1}}{2h_{i+1}^2}$$

$$+ \frac{\sigma_0^2}{h_{i+1}^2}\frac{s_{i+1}^{2\gamma+3}}{2(2\gamma+3)} - \frac{r(s_{i+1}+2s_i)}{6} \tag{44}$$

$$a^3_{i,\,i+1} = rm^1_{i+1} = \frac{rh_{i+1}}{6} \tag{45}$$

Its diagonal elements $a_{i,\,i}$ will contain the following integrals (note that $\frac{\partial\varphi_i}{\partial s} = \frac{1}{h_i}\,\forall\, s \in (s_{i-1},\, s_i)$ and $\frac{\partial\varphi_i}{\partial s} = -\frac{1}{h_{i+1}}\,\forall\, s\, \in (s_i,\, s_{i+1}))$

$$\begin{aligned} a^1_{i,\,i} &= \frac{\sigma_0^2}{2}\int_0^{S_b} s^{2\gamma+2}(\frac{\partial\varphi_i}{\partial s})^2 ds = \frac{\sigma_0^2}{2}(\int_{s_{i-1}}^{s_i} \frac{s^{2\gamma+2}}{h_i^2} ds) \\ &\quad + \frac{\sigma_0^2}{2}\int_{s_i}^{s_{i+1}} \frac{s^{2\gamma+2}}{h_{i+1}^2} ds \\ &= \frac{\sigma_0^2}{2h_i^2}(\frac{s_i^{2\gamma+3} - s_{i-1}^{2\gamma+3}}{2\gamma+3}) + \frac{\sigma_0^2}{2h_{i+1}^2}(\frac{s_{i+1}^{2\gamma+3} - s_i^{2\gamma+3}}{2\gamma+3}) \end{aligned} \tag{46}$$

$$\begin{aligned} a^2_{i,\,i} &= (1+\gamma)\sigma_0^2\int_0^{S_b} s^{2\gamma+1}\varphi_i\frac{\partial\varphi_i}{\partial s} ds - r\int_0^{S_b} s\varphi_i\frac{\partial\varphi_i}{\partial s}\, ds \\ &= \frac{(1+\gamma)\sigma_0^2}{h_i^2}(\frac{s_i^{2\gamma+3}}{2\gamma+3} - \frac{s_i^{2\gamma+2}s_{i-1}}{2\gamma+2} + \frac{s_{i-1}^{2\gamma+3}}{(2\gamma+2)(2\gamma+3)}) \\ &\quad - \frac{(1+\gamma)\sigma_0^2}{h_{i+1}^2}(\frac{s_{i+1}^{2\gamma+3}}{(2\gamma+3)(2\gamma+2)} - \frac{s_i^{2\gamma+2}s_{i+1}}{2\gamma+2} + \frac{s_i^{2\gamma+3}}{2\gamma+3}) \\ &\quad - \frac{r}{h_i^2}(\frac{s_i^3}{3} - \frac{s_i^2 s_{i-1}}{2} + \frac{s_{i-1}^3}{6}) + \frac{r}{h_{i+1}^2}(\frac{s_{i+1}^3}{6} - \frac{s_i^2 s_{i+1}}{2} + \frac{s_i^3}{3}) \\ &= \frac{(1+\gamma)\sigma_0^2}{h_i^2}(\frac{s_i^{2\gamma+3}}{2\gamma+3} - \frac{s_i^{2\gamma+2}s_{i-1}}{2\gamma+2}) + \frac{\sigma_0^2}{h_i^2}\frac{s_{i-1}^{2\gamma+3}}{2(2\gamma+3)} \\ &\quad - \frac{(1+\gamma)\sigma_0^2}{h_{i+1}^2}(-\frac{s_i^{2\gamma+2}s_{i+1}}{2\gamma+2} + \frac{s_i^{2\gamma+3}}{2\gamma+3}) \\ &\quad - \frac{\sigma_0^2}{h_{i+1}^2}\frac{s_{i+1}^{2\gamma+3}}{2(2\gamma+3)} + \frac{r(h_i+h_{i+1})}{6} \end{aligned} \tag{47}$$

$$a^3_{i,\,i} = rm_{i,i} = r(\frac{h_i + h_{i+1}}{3}) \tag{48}$$

From equations (**32**) – (**46**), we can calculate the entries of A as follows (remember that A is a tridiagonal matrix)

$$a_{i,\,i-1} \;=\; a^1_{i,\,i-1} + a^2_{i,\,i-1} + a^3_{i,\,i-1} = -\frac{\sigma_0^2}{2h_i^2}\Big(\frac{s_i^{2\gamma+3} - s_{i-1}^{2\gamma+3}}{2\gamma+3}\Big)$$

$$-\frac{(1+\gamma)\sigma_0^2}{h_i^2}\frac{s_i^{2\gamma+3}}{2\gamma+3} + \frac{\sigma_0^2}{h_i^2}\frac{s_i^{2\gamma+2}s_{i-1}}{2}$$

$$-\frac{\sigma_0^2 s_{i-1}^{2\gamma+3}}{2h_i^2(2\gamma+3)} + \frac{r(2s_i + s_{i-1})}{6} + r\frac{h_i}{6}$$

$$= \frac{-\sigma_0^2 s_i^{2(\gamma+1)}}{2h_i} \;+\; \frac{rs_i}{2} \quad \forall \;\; 1 \le i \le N_s \tag{49}$$

$$a_{i,\,i+1} \;=\; a^1_{i,\,i+1} + a^2_{i,\,i+1} + a^3_{i,\,i+1} = \frac{-\sigma_0^2}{2h_{i+1}^2}\Big(\frac{s_{i+1}^{2\gamma+3} - s_i^{2\gamma+3}}{2\gamma+3}\Big)$$

$$+\frac{\sigma_0^2}{h_{i+1}^2}\frac{s_{i+1}^{2\gamma+3}}{2(2\gamma+3)} - \frac{\sigma_0^2 s_i^{2\gamma+2}s_{i+1}}{2h_{i+1}^2}$$

$$+\frac{(1+\gamma)\sigma_0^2 s_i^{2\gamma+3}}{h_{i+1}^2(2\gamma+3)} - \;\frac{r(s_{i+1}+2s_i)}{6} \;+\; r\frac{h_{i+1}}{6}$$

$$= \frac{-s_i^{2(\gamma+1)}\sigma_0^2}{2h_{i+1}} \;-\; \frac{rs_i}{2} \quad \forall \;\; 0 \le i \le N_s - 1 \tag{50}$$

$$a_{0,0} \;=\; a^1_{0,\,0} + a^2_{0,\,0} + a^3_{0,\,0} = \frac{\sigma_0^2 s_1^{1+2\gamma}}{2(3+2\gamma)}$$

$$-\frac{\sigma_0^2 s_1^{1+2\gamma}}{2(3+2\gamma)} + \frac{rs_1}{6} + \frac{rh_1}{3} = \frac{rs_1}{2} \tag{51}$$

$$a_{N_s,\,N_s} \;=\; a^1_{N_s,\,N_s} + a^2_{N_s,\,N_s} + a^3_{N_s,\,N_s}$$

$$= \frac{(1+\gamma)\sigma_0^2}{h_{N_s}^2}\Big(\frac{s_{N_s}^{2\gamma+3}}{2\gamma+3} - \frac{s_{N_s}^{2\gamma+2}s_{N_s-1}}{2\gamma+2}\Big)$$

$$+\frac{\sigma_0^2}{2h_{N_s}^2}\Big(\frac{s_{N_s}^{3+2\gamma} - s_{N_s-1}^{3+2\gamma}}{3+2\gamma}\Big) + \;\frac{rh_{N_s}}{3}$$

$$+\frac{\sigma_0^2 s_{N_s-1}^{2\gamma+3}}{2h_{N_s}^2(2\gamma+3)} - \frac{r(2s_{N_s}+s_{N_s-1})}{6}$$

$$= \frac{s_{N_s}^{2(\gamma+1)}\sigma_0^2}{2h_{N_s}} - \frac{rs_{N_s-1}}{2} \tag{52}$$

$$a_{i,i} = a_{i,i}^1 + a_{i,i}^2 + a_{i,i}^3 = \frac{\sigma_0^2}{2h_i^2}(\frac{s_i^{2\gamma+3}-s_{i-1}^{2\gamma+3}}{2\gamma+3})$$

$$+\frac{(1+\gamma)\sigma_0^2}{h_i^2}(\frac{s_i^{2\gamma+3}}{2\gamma+3} - \frac{s_i^{2\gamma+2}s_{i-1}}{2\gamma+2})$$

$$+\frac{\sigma_0^2}{2h_{i+1}^2}(\frac{s_{i+1}^{2\gamma+3}-s_i^{2\gamma+3}}{2\gamma+3}) + \frac{\sigma_0^2 s_{i-1}^{2\gamma+3}}{2h_i^2(2\gamma+3)}$$

$$-\frac{(1+\gamma)\sigma_0^2}{h_{i+1}^2}(-\frac{s_i^{2\gamma+2}s_{i+1}}{2\gamma+2} + \frac{s_i^{2\gamma+3}}{2\gamma+3})$$

$$+\frac{r(h_i+h_{i+1})}{6} + \frac{r(h_i+h_{i+1})}{3} + \frac{\sigma_0^2 s_{i+1}^{2\gamma+3}}{2h_{i+1}^2(2\gamma+3)}$$

$$= \frac{s_i^{2(\gamma+1)}\sigma_0^2}{2}(\frac{1}{h_i}+\frac{1}{h_{i+1}})$$

$$+\frac{r(h_i+h_{i+1})}{2} \quad \forall \quad 1 \le i \le N_s - 1 \tag{53}$$

In summary, we get the form of the stiffness and mass matrices, A and M, rspectively (note that the entries of matrices$A$ and M don't depend on time, which is k, in this case) :

$$A := \begin{pmatrix} a_{0,0} & a_{0,1} & 0 & ... & 0 \\ a_{1,0} & ... & ... & ... & 0 \\ 0 & ... & ... & ... & ... \\ ... & ... & ... & ... & a_{N_s-1,N_s} \\ 0 & 0 & ... & a_{N_s,N_s-1} & a_{N_s,N_s} \end{pmatrix}$$

where $a_{0,0}$, $a_{0,1}$, a_{N_s-1,N_s}, $a_{1,0}$, a_{N_s,N_s-1} and a_{N_s,N_s} are given by the formulas $(49)-(53)$ with $i = 1$ and $N_s - 1$

$$M := \begin{pmatrix} \frac{h_1}{3} & \frac{h_1}{6} & 0 & 0 & 0 \\ \frac{h_1}{6} & \frac{h_1+h_2}{3} & \frac{h_2}{6} & \dots & \dots \\ 0 & \frac{h_2}{6} & \dots & \dots & 0 \\ \dots & \dots & \dots & \frac{h_{N_s-1}+h_{N_s}}{3} & \frac{h_{N_s}}{6} \\ 0 & 0 & \dots & \frac{h_{N_s}}{6} & \frac{h_{N_s}}{3} \end{pmatrix}$$

For an equidistant grid in the S-direction (that is, uniform partition), implying $h := h_1 = \ldots = h_{N_s}$, the matrices can be simplified further, which further on will reduce the cost of calculation. On the non-equidistant grid, with A and M defined as in (**23**) and (**24**), the required time of calculation increases proportionally for higher fineness of the mesh (larger k). Thus when a non-equidistant lattice is used, it should be designed in a manner that good accuracy will be achieve for a relatively small amount of grid points.

Note that matrix $M + \frac{\triangle t_k}{2} A$ can be further reduced by omitting the first row and first column due to the two boundary conditions $u_h^0 = max(K-s,\, 0)$ and $u_h(0,\, t_k) = Ke^{-rt_k}$. These boundary values are each interpolated by one hat function with the corresponding coefficients $u_{h,\,0}^{k=0,1,\ldots,\,N_t}$ and $u_{h,\,i=1,\ldots,\,N_s}^{0}$. This means these coefficients are known and we only have N_s unknown coefficients left. Hence, we may cancel the first column and row of matrix $M + \frac{\triangle t_k}{2} A$, the first row of matrix $(M - \frac{\triangle t_k}{2} A)\, u_h^{k-1}$ and the first element of vectors u_h^k. The matrix $(M + \frac{\triangle t_k}{2} A)$ now has size $N_s \times N_s$, $(M - \frac{\triangle t_k}{2} A)\, u_h^{k-1}$ has size $N_s \times 1$ and vector u_h^k now has size $N_s \times 1$. The boundary terms that were dropped during this reduction process are put into a vector c^k with size $N_s \times 1$, and the final system of equations will have the following form:

$$(M + \frac{\triangle t_k}{2} A) u_h^k = (M - \frac{\triangle t_k}{2} A) u_h^{k-1} - c^k \tag{54}$$

in which $c^k = \begin{pmatrix} (\frac{h_1}{6} + \frac{\triangle t_k}{2} a_{1,\,0})\, u_{h,\,0}^k \\ 0 \\ \dots \\ 0 \\ 0 \end{pmatrix}$ and $u_h^k = \begin{pmatrix} u_{h,\,1}^k \\ u_{h,\,2}^k \\ \dots \\ u_{h,\,N_s-1}^k \\ u_{h,\,N_s}^k \end{pmatrix}$.

The linear system of equations (**54**) is equivalent to one with homogeneous boundary conditions where the function vanishes on the boundary. We can rewrite the linear of system of equations (**54**) in the form
$Eu_h^k = Fu_h^{k-1} - c^k$, and the entries of matrices E and F are below, respectively

$$e_{i,i-1} = \frac{\triangle t_k}{2}(\frac{-\sigma_0^2 s_i^{2(\gamma+1)}}{2h_i} + \frac{rs_i}{2}) + \frac{h_i}{6},\ 2 \le i \le N_s$$

$$e_{i,i} = \frac{\triangle t_k}{2}(\frac{s_i^{2(\gamma+1)}\sigma_0^2}{2}(\frac{1}{h_i} + \frac{1}{h_{i+1}}) + \frac{r(h_i + h_{i+1})}{2}) + \frac{h_i + h_{i+1}}{3},\ 1 \le i \le N_s - 1$$

$$e_{i,i+1} = \frac{\triangle t_k}{2}(\frac{-s_i^{2(\gamma+1)}\sigma_0^2}{2h_{i+1}} - \frac{rs_i}{2}) + \frac{h_{i+1}}{6},\ 1 \le i \le N_s - 1$$

$$e_{N_s,N_s} = \frac{\triangle t_k}{2}(\frac{s_{N_s}^{2(\gamma+1)}\sigma_0^2}{2h_{N_s}} - \frac{rs_{N_s-1}}{2}) + \frac{h_{N_s}}{3}$$

$$f_{i,i-1} = \frac{-\triangle t_k}{2}(\frac{-\sigma_0^2 s_i^{2(\gamma+1)}}{2h_i} + \frac{rs_i}{2}) + \frac{h_i}{6},\ 2 \le i \le N_s$$

$$f_{i,i} = \frac{-\triangle t_k}{2}(\frac{s_i^{2(\gamma+1)}\sigma_0^2}{2}(\frac{1}{h_i} + \frac{1}{h_{i+1}}) + \frac{r(h_i + h_{i+1})}{2}) + \frac{h_i + h_{i+1}}{3},\ 1 \le i \le N_s - 1$$

$$f_{i,i+1} = \frac{-\triangle t_k}{2}(\frac{-s_i^{2(\gamma+1)}\sigma_0^2}{2h_{i+1}} - \frac{rs_i}{2}) + \frac{h_{i+1}}{6},\ 1 \le i \le N_s - 1$$

$$e_{N_s,N_s} = \frac{-\triangle t_k}{2}(\frac{s_{N_s}^{2(\gamma+1)}\sigma_0^2}{2h_{N_s}} - \frac{rs_{N_s-1}}{2}) + \frac{h_{N_s}}{3}$$

With those formulas and the given value of $u_h^0 = max(K-s,\, 0)$, we can compute iteratively the unknown variables $u_{h,\,i}^k$ for $i = 1, 2, \ldots,\, N_s,$ and $k = 1, 2, \ldots,\, N_t$, and obtain the prices of our put option for any given values of both time $t \in [0,\, 1]$ and the underlying asset $s \in [0,\, S_b]$.

Note that although we choose geometric partition in the S-direction, we decide to employ two ways of partition for the time interval $[0, 1]$ into N_t subintervals with $\triangle t_k = t_k - t_{k-1}$ for $k = 1, \ldots, N_t$: uniform or geometric partition, in order to see which partition gives a higher accuracy. Both partitions are exactly the same as those used in the S-direction, which means for the geometric partition, the number of points t_i around $t = 0$ increase significantly. However, although the geometric partition increases the cost of computation, the errors of our numerical solutions in this case are much larger than those obtained in the case of uniform partition. Therefore, for discretizing our mesh in the T-direction, it is best to choose the uniform partition to increase the accurracy of our numerical solutions while reducing the computation time required, especially for cases when σ_0 and γ are sufficiently small (for example, $\sigma_0 = 0.3$ and $\gamma = -0.03$)

2.4 Galerkin Least squares stabilization Method

Theoretically, the local volatility σ can be any positive values, but in practice, the local volatility of an option may be abnormally large due to some unexpectedly horrible news or events that occur (for example, in 2008, after Lehman Brothers and Bear Sterns collapsed, the Down Jones closed down just over 500 points at the time the largest drop by points in a single day since the days following the attacks on September 11, 2001, or in Japan, banks and insurers announced a combined 249 billion yen ($2.4 billion) in losses due to this collapse). The impacts of such events will increase volatility of option prices significantly, and such cases correspond to sufficiently large vales of σ_0 and γ (for example, $\sigma_0 = 0.7$ and $\gamma = 0.05$). We realize that the presented Galerkin FEM does not work well for large local volatility due to its high sensitivity to the large values of σ_0. One way to fix this problem is to apply the Least Square Regression (LSR) method, but it has one major drawback: the solution is much harder to compute by iterative methods and more sensitive to roundoff errors since the number of

matrices in the equation (**22**) scales as the square of the number of the matrix in the Ritz - Galerkin method. The LSR method is also less accurate in the regions where the solution is smooth. Thus, we decide to combine the Least Square and Ritz- Galerkin methods together, called the Galerkin Least Square (GLS) method, by adding an additional "Least Square" term to the LHS of equation (**22**), which is equivalent to one of the two options belows:

1. $(\frac{\partial u}{\partial t},\, \varphi) + (\alpha \frac{\partial u}{\partial s},\, \frac{\partial \varphi}{\partial s}) + (\beta \frac{\partial u}{\partial s},\, \varphi) + (ru,\, \varphi) + \sum_{\tau \in T_h} (\frac{\partial u}{\partial t} - \frac{\partial}{\partial s}(\alpha \frac{\partial u}{\partial s}) + \beta \frac{\partial u}{\partial s} + ru,\, \rho_i(-\frac{\partial}{\partial s}(\alpha \frac{\partial \varphi}{\partial s}) + \beta \frac{\partial \varphi}{\partial s} + r\varphi)) = 0$
2. $(\frac{\partial u}{\partial t},\, \varphi) + (\alpha \frac{\partial u}{\partial s},\, \frac{\partial \varphi}{\partial s}) + (\beta \frac{\partial u}{\partial s},\, \varphi) + (ru,\, \varphi) + \sum_{\tau \in T_h} (\frac{\partial u}{\partial t} - \frac{\partial}{\partial s}(\alpha \frac{\partial u}{\partial s}) + \beta \frac{\partial u}{\partial s} + ru,\, \rho_i(-\frac{\partial}{\partial s}(\alpha \frac{\partial \varphi}{\partial s}) + \beta \frac{\partial \varphi}{\partial s})) = 0$

in which the stability parameter ρ_i is defined locally based on the Peclet number $Pe_i(\frac{s_i+s_{i+1}}{2}) = \frac{h_{T_h}|b(\frac{s_i+s_{i+1}}{2})|_p}{24\epsilon}$ on each partition τ as follows,

$$\rho_i(s,\, Pe_i(\frac{s_i+s_{i+1}}{2})) = \begin{cases} \frac{h_{T_i}^2}{48\epsilon}, & 0 \le Pe_i(\frac{s_i+s_{i+1}}{2}) < 1 \\ \frac{h_{T_i}}{2|b(\frac{s_i+s_{i+1}}{2})|_p}, & Pe_i(\frac{s_i+s_{i+1}}{2}) \ge 1 \end{cases} \tag{55}$$

$$|b(\frac{s_i+s_{i+1}}{2})|_p = \begin{cases} (\sum_{i=1}^{N} |b_i(\frac{s_i+s_{i+1}}{2})|_p)^{\frac{1}{p}}, & 1 \le p < \infty \\ max_{i=1,..,N} |b_i(\frac{s_i+s_{i+1}}{2})|, & p = \infty \end{cases} \tag{56}$$

After discretizing the equation (**22**) in space, time (dividing the interval $[0, 1]$ into N_t subintervals $[t_k,\, t_{k-1}]$, $k = 1, \ldots, N_t$ with lengths $\triangle t_k = t_k - t_{k-1}$) and rewriting $u_h(s,\, t_k) = \sum_{i=1}^{2} u_{h,\,i}(t_k)\varphi_i(s)$, where φ_i is again the linear test function of V_h^b, we again obtain the stabilized fully discrete variational problem:

Find $u_h(s,\, t_k) \in V_h^b$ such that

$$M^{LQ}(u_h^k,\, \varphi) + A^{LQ}(u_h^k,\, \varphi) = 0 \;\; \forall\, \varphi \in V_h^b \;\; \text{and} \;\; t_k \in [0,\, 1], \tag{57}$$

where

$$m^{LQ}(u_h^k,\, \varphi) \;= (u_h^k,\, \varphi) + \sum_{\tau \in T_h} (\frac{\partial u_h^k}{\partial t},\, \rho_i(-\varepsilon \frac{\partial}{\partial s}(\alpha \frac{\partial \varphi}{\partial s}) + \beta \frac{\partial \varphi}{\partial s} + r\varphi)) \qquad (58)$$

is an augmented inertial form of the mass matrix M^{LQ}, and

$$a^{LQ}(u_h^k,\, \varphi) \;=\; (\alpha \frac{\partial u_h^k}{\partial s},\, \frac{\partial \varphi}{\partial s}) + (\beta \frac{\partial u_h^k}{\partial s},\, \varphi) + (r u_h^k,\, \varphi)$$

$$+ \sum_{\tau \in T_h} (-\frac{\partial}{\partial s}(\alpha \frac{\partial u_h^k}{\partial s}) + \beta \frac{\partial u_h^k}{\partial s} + r u_h^k,\, \rho_i(-\varepsilon \frac{\partial}{\partial s}(\alpha \frac{\partial \varphi}{\partial s}) + \beta \frac{\partial \varphi}{\partial s} + r\varphi)) \qquad (59)$$

is a stabilized Galerkin form of the stiffnex matrix A^{LQ}. In this formula, ε are either 0,1 or -1, which corresponds to the SUPG, GLS and MS method, respectively. We will fully solve the problem using option 1's formulation ($\varepsilon = 1$), which is the most intense computational case. Without repetition, we only present the general formula to form matrices M^{LQ} and A^{LQ} in the case of option (**2**).

Given $u_h^0 = max(K - s,\, 0)$, by using the Crank-Nicolson scheme corresponding to the values of $\theta = \frac{1}{2}$, we can find u_h^{k+1} for $k = 0, 1, \ldots, N_t - 1$ from the following equation

$$\frac{1}{\triangle t_k} m^{LQ}(u_h^k - u_h^{k-1},\, \varphi) \;+\; a^{LQ}(\theta u_h^k + (1-\theta) u_h^{k-1},\, \varphi) \;= 0 \;\forall\; \varphi \in V_h^b \qquad (60)$$

Let $(\varphi_i)_{i=0,\ldots,N_s}$ be the basis, or hat functions in V_h, and let M^{LQ} be the mass matrix whose entries are defined by

$$m_{i,\,j}^{LQ} = (\varphi_j,\, \varphi_i) + \sum_{\tau \in T_h} \rho_i[(\varphi_j,\, r\varphi_i) - (\varphi_j,\, rs \frac{\partial \varphi_i}{\partial s})] \qquad (61)$$

since φ is the hat functions and $\alpha \frac{\partial^2 \varphi}{\partial s^2} = 0$, $\frac{\partial}{\partial s}(\alpha \frac{\partial \varphi}{\partial s}) + \beta \frac{\partial \varphi}{\partial s} = -rs$. Futhermore, let $\sum_{\tau \in T_h} \rho_i(\varphi_j,\, r\varphi_i) = m_{i,\,j}^{LQ,\,1}$ and $\sum_{\tau \in T_h} \rho_i(\varphi_j,\, rs \frac{\partial \varphi^i}{\partial s}) = m_{i,\,j}^{LQ,\,2}$, we can rewrite equation (**59**) as

$$m_{i,j}^{LQ} = (\varphi_j,\, \varphi_i) + m_{i,j}^{LQ,1} - m_{i,j}^{LQ,2} \tag{62}$$

Since $a\,(\varphi_j,\, \varphi_i) = (\alpha\frac{\partial\varphi_j}{\partial s},\, \frac{\partial\varphi_i}{\partial s}) + (\beta\frac{\partial\varphi_j}{\partial s},\, \varphi_i) + (r\varphi_j,\, \varphi_i)$ as defined in equation (**22**), the entries of the stiffness matrix A^{LQ} are given as

$$a_{i,,j}^{LQ} = a\,(\varphi_j,\, \varphi_i) + \sum_{\tau\in T_h} \rho_i[(r\varphi_j,\, r\varphi_i) - (rs\frac{\partial\varphi_j}{\partial s},\, r\varphi_i) + (rs\frac{\partial\varphi_j}{\partial s},\, rs\frac{\partial\varphi_i}{\partial s})]$$

$$- \sum_{\tau\in T_h} \rho_i(r\varphi_j,\, rs\frac{\partial\varphi_i}{\partial s}), \quad \forall\, 0 \le i,\, j \le N_s. \tag{63}$$

From the following identities,

$$\sum_{\tau\in T_h} \rho_i(r\varphi_j,\, r\varphi_i) \;= rm_{i,j}^{LQ,1}$$

,

$$\sum_{\tau\in T_h} \rho_i(rs\frac{\partial\varphi_j}{\partial s},\, rs\frac{\partial\varphi_i}{\partial s}) \quad = \sum_{\tau\in T_h} \rho_i\frac{r^2 a_{i,j}^{LQ,1}}{\sigma^2}$$

$$\sum_{\tau\in T_h} \rho_i(rs\frac{\partial\varphi_j}{\partial s},\, r\varphi_i) \qquad = \sum_{\tau\in T_h} \rho_i\frac{r^2 a_{i,j}^{LQ,2}}{-r+\sigma^2}$$

$$\sum_{\tau\in T_h} \rho_i(r\varphi_j,\, rs\frac{\partial\varphi_i}{\partial s}) \;= rm_{i,j}^{LQ,2}.$$

the equation (**59**) is equivalent to

$$a_{i,j}^{LQ} = a\,(\varphi_j,\, \varphi_i) + rm_{i,j}^{LQ,1} + \sum_{\tau\in T_h} \rho_i[-\frac{r^2 a_{i,j}^{LQ,2}}{-r+\sigma^2} + \frac{r^2 a_{i,j}^{LQ,1}}{\frac{\sigma^2}{2}}] - rm_{i,j}^{LQ,2}$$

By letting $u_h^k = \left(u_h^k\,(s_0), \ldots,\, u_h^k\,(s_N)\right)^T$ and $u_h^0 = \left(u_h^0\,(s_0), \ldots,\, u_h^0\,(s_N)\right)^T$ which is the boundary condition, the fully discrete problem (**60**) can be rewritten as a system of linear equations

$$(M^{LQ} + \frac{\triangle t_k}{2}A^{LQ})u_h^k \;= (M^{LQ} - \frac{\triangle t_k}{2}A^{LQ})u_h^{k-1} \tag{64}$$

We now compute the following general formula for the stiffness matrix M^{LQ}. By using equation (**62**), we need to compute the following elements

$$m_{i,\,i-1}^{LQ,\,2} = r\int_0^{S_b} s\varphi_{i-1}\frac{\partial\varphi_i}{\partial s}ds \;= \rho_{i-1}r(\frac{s_i}{6}+\frac{s_{i-1}}{3})$$

$$m_{i,\,i+1}^{LQ,\,2} \;= r\int_0^{S_b} s\varphi_{i+1}\frac{\partial\varphi_i}{\partial s}ds \;= -\,\rho_{i-1}r(\frac{s_{i+1}}{3}+\frac{s_i}{6})$$

$$m_{0,\,0}^{LQ,\,2} = r\int_0^{S_b} s\varphi_0\frac{\partial\varphi_0}{\partial s}ds = -\,\frac{\rho_0 r h_1}{6}$$

$$m_{N_s,\,N_S}^{LQ,\,2} = r\int_0^{S_b} s\varphi_{N_s}\frac{\partial\varphi_{N_s}}{\partial s}ds$$

$$= \rho_{N_s-1}r(\frac{s_{N_s-1}}{6}+\frac{s_{N_s}}{3})$$

$$m_{i,\,i}^{LQ,\,2} \;= r\int_0^{S_b} s\varphi_i\frac{\partial\varphi_i}{\partial s}ds = r(\frac{\rho_{i-1}(2s_i+s_{i-1})}{6})$$

$$-\,r\frac{\rho_i(2s_i+s_{i+1})}{6}$$

Together with the formulas (**30**) $-$ (**34**), the entries of M are given as follows

$$m_{i,\,i-1}^{LQ} = (\varphi_{i-1},\,\varphi_i) + m_{i,\,i-1}^{LQ,\,1} - m_{i,\,i-1}^{LQ,\,2} = \frac{h_i}{6} + \rho_{i-1}r\frac{h_i}{6}$$

$$-\,\rho_{i-1}r(\frac{s_i}{6}+\frac{s_{i-1}}{3})$$

$$= \frac{h_i}{6} \;-\; \frac{\rho_{i-1}s_{i-1}r}{2},\;\forall\, 1\le i\le N_s$$

$$m_{i,\,i+1}^{LQ} = (\varphi_{i+1},\,\varphi_i) + m_{i,\,i+1}^{LQ,\,1} - m_{i,\,i+1}^{LQ,\,2} = \frac{h_{i+1}}{6} + \rho_i r\frac{h_{i+1}}{6}$$

$$-\,\rho_i r(-\frac{s_{i+1}}{3}-\frac{s_i}{6})$$

$$= \frac{h_{i+1}}{6} + \frac{\rho_i s_{i+1} r}{2},\ 0 \le i \le N_s - 1$$

$$m_{0,0}^{LQ} = (\varphi_0,\, \varphi_0) + m_{0,0}^{LQ,1} - m_{0,0}^{LQ,2} = \frac{h_1}{3} + \rho_0 r \frac{h_1}{3}$$

$$+ \frac{\rho_0 r h_1}{6} = \frac{h_1}{3} + \frac{\rho_0 h_1 r}{2} \tag{65}$$

$$m_{N_s,\,N_s}^{LQ} = (\varphi_{N_s},\, \varphi_{N_s}) + m_{N_s,\,N_s}^{LQ,1} - m_{N_s,\,N_s}^{LQ,2}$$

$$= \frac{h_{N_s}}{3} + \rho_{N_s-1} r \frac{h_{N_s}}{3}$$

$$- \rho_{N_s-1} r (\frac{s_{N_s-1}}{6} + \frac{s_{N_s}}{3})$$

$$= \frac{h_{N_s}}{3} - \frac{\rho_{N_s-1} r s_{N_s-1}}{2} \tag{66}$$

$$m_{i,i}^{LQ} = (\varphi_i,\, \varphi_i) + m_{i,i}^{LQ,1} - m_{i,i}^{LQ,2} = \frac{h_i + h_{i+1}}{3} + r \frac{\rho_{i-1} h_i + \rho_i h_{i+1}}{3}$$

$$- r \frac{\rho_{i-1}(2s_i + s_{i-1})}{6} - r \frac{\rho_{i-1}(2s_i + s_{i-1})}{6}$$

$$+ r \frac{\rho_i (2s_i + s_{i+1})}{6}$$

$$= (\frac{-r s_{i-1} \rho_{i-1}}{2} + \frac{h_i}{3}) + (\frac{r s_{i+1} \rho_i}{2} + \frac{h_{i+1}}{3}),\ 1 \le i \le N_s - 1 \tag{67}$$

Similarly, the entries of A are given as

$$a_{i,\,i-1}^{LQ} = a\,(\varphi_{i-1},\, \varphi_i) + r m_{i,\,i-1}^{LQ,1} + \sum_{\tau \in T_h} \rho_i [- \frac{r^2 a_{i,\,i-1}^{LQ,2}}{-r + \sigma^2} + \frac{r^2 a_{i,\,i-1}^{LQ,1}}{\frac{\sigma^2}{2}}]$$

$$- r m_{i,\,i-1}^{LQ,2} = \frac{-\sigma_0^2 s_i^{2(\gamma+1)}}{2h_i} + \frac{r s_i}{2}$$

$$+ r^2\rho_{i-1}\frac{h_i}{6} \; + \; \rho_{i-1}r^2\frac{s_{i-1}}{6} \; + \; \rho_{i-1}r^2\frac{s_i}{3}$$

$$- \rho_{i-1}r^2(\frac{s_i - s_{i-1}}{3} + \frac{s_i s_{i-1}}{h_i}) \; - \; \rho_{i-1}r^2(\frac{s_i}{6} + \frac{s_{i-1}}{3})$$

$$= \frac{-\rho_{i-1}r^2 s_i s_{i-1}}{h_i} \; - \; \frac{\sigma_0^2 s_i^{2(\gamma+1)}}{2h_i} \; + \; \frac{rs_i}{2}, \quad 1 \le i \le N_s \tag{68}$$

$$a_{i,\,i+1}^{LQ} = a\left(\varphi_{i+1},\, \varphi_i\right) + rm_{i,\,i+1}^{LQ,\,1} + \sum_{\tau \in T_h} \rho_i[-\frac{r^2 a_{i,\,i+1}^{LQ,\,2}}{-r + \sigma^2} + \frac{r^2 a_{i,\,i+1}^{LQ,\,1}}{\frac{\sigma^2}{2}}]$$

$$- rm_{i,\,i+1}^{LQ,\,2} = \frac{-s_i^{2(\gamma+1)}\sigma_0^2}{2h_{i+1}} \; - \; \frac{rs_i}{2}$$

$$+ r^2\rho_i\frac{h_{i+1}}{6} \; - \; r^2\rho_i(\frac{s_{i+1}}{6} + \frac{s_i}{3})$$

$$- r^2\rho_i(\frac{s_{i+1} - s_i}{3} + \frac{s_i s_{i+1}}{h_{i+1}}) + \; r^2\rho_i(\frac{s_{i+1}}{3} + \frac{s_i}{6})$$

$$= \frac{-\rho_i r^2 s_i s_{i+1}}{h_{i+1}} \; - \; \frac{s_i^{2(\gamma+1)}\sigma_0^2}{2h_{i+1}} \; - \; \frac{rs_i}{2}, \quad 0 \le i \le N_s - 1$$

$$a_{0,\,0}^{LQ} = a\left(\varphi_0,\, \varphi_0\right) + rm_{0,\,0}^{LQ,\,1} + \sum_{\tau \in T_h} \rho_i[-\frac{r^2 a_{0,\,0}^{LQ,\,2}}{-r + \sigma^2} + \frac{r^2 a_{0,\,0}^{LQ,\,1}}{\frac{\sigma^2}{2}}]$$

$$-rm_{0,\,0}^{LQ,\,2} = \frac{rs_1}{2} \; + \; r^2\rho_0\frac{h_1}{3} \; + \; r^2\rho_0\frac{h_1}{6}$$

$$+ r^2\rho_0\frac{h_1}{3} \; + \; r^2\rho_0\frac{h_1}{6} \; = p_0 h_1 r^2 + \frac{rs_1}{2} \tag{69}$$

$$a_{N_s,\,N_s}^{LQ} = \sum_{\tau \in T_h} \rho_i[-\frac{r^2 a_{N_s,\,N_s}^{LQ,\,2}}{-r + \sigma^2} + \frac{r^2 a_{N_s,\,N_s}^{LQ,\,1}}{\frac{\sigma^2}{2}}]$$

$$+ rm_{N_s,\,N_s}^{LQ,\,1} - rm_{N_s,\,N_s}^{LQ,\,2}$$

$$+a\left(\varphi_{N_s},\,\varphi_{N_s}\right)$$

$$= \frac{s_{N_s}^{2(\gamma+1)}\sigma_0^2}{2h_{N_s}} - \frac{rs_{N_s-1}}{2} + r^2\rho_{N_s-1}\frac{h_{N_s}}{3}$$

$$- r^2\rho_{N_s-1}(\frac{s_{N_s-1}}{6} + \frac{s_{N_s}}{3})$$

$$+ r^2\rho_{N_s-1}(\frac{h_{N_s}}{3} + \frac{s_{N_s}s_{N_s-1}}{h_{N_s}})$$

$$- \rho_{N_s-1}r^2(\frac{s_{N_s-1}}{6} + \frac{s_{N_s}}{3}) = \frac{\rho_{N_s-1}r^2 s_{N_s}s_{N_s-1}}{h_{N_s}}$$

$$+ \frac{s_{N_s}^{2(\gamma+1)}\sigma_0^2}{2h_{N_s}} - \frac{rs_{N_s-1}}{2} - r^2\rho_{N_s-1}s_{N_s-1} \tag{70}$$

$$a_{i,\,i}^{LQ} = a\left(\varphi_i,\,\varphi_i\right) + \sum_{\tau\in T_h}\rho_i[-\frac{r^2a_{i,\,i}^{LQ,\,2}}{-r+\sigma^2} + \frac{r^2a_{i,\,i}^{LQ,\,1}}{\frac{\sigma^2}{2}}]$$

$$+rm_{i,\,i}^{LQ,\,1} - rm_{i,\,i}^{LQ,\,2}$$

$$= \frac{s_i^{2(\gamma+1)}\sigma_0^2}{2}(\frac{1}{h_i} + \frac{1}{h_{i+1}}) + \frac{r(h_i+h_{i+1})}{2}$$

$$+ r^2(\frac{\rho_{i-1}h_i + \rho_i h_{i+1}}{3}) - r^2\frac{\rho_{i-1}(2s_i + s_{i-1})}{6}$$

$$+ r^2\frac{\rho_i(2s_i + s_{i+1})}{6} + r^2\rho_{i-1}(\frac{h_i}{3} + \frac{s_is_{i-1}}{h_i})$$

$$+ r^2\rho_i(\frac{h_{i+1}}{3} + \frac{s_is_{i+1}}{h_{i+1}}) - r^2(\frac{\rho_{i-1}(2s_i + s_{i-1})}{6})$$

$$+ r^2\frac{\rho_i(2s_i + s_{i+1})}{6}$$

$$= (s_{i+1}\rho_i r^2 + s_i r^2\frac{\rho_i s_{i+1}}{h_{i+1}}) + (s_i r^2\frac{\rho_{i-1}s_{i-1}}{h_i} - r^2 s_{i-1}\rho_{i-1})$$

$$+\frac{s_i^{2(\gamma+1)}\sigma_0^2}{2}(\frac{1}{h_i}+\frac{1}{h_{i+1}})$$

$$+\frac{r(h_i+h_{i+1})}{2},\ 1\le i\le N_s-1 \tag{71}$$

Note that matrix $M^{LQ}+\frac{\triangle t_k}{2}A^{LQ}$ can be further reduced by omitting the first row and first column due to the two boundary conditions $u_h^0=max(K-s,\,0)$ and $u_h(0,\,t_k)=Ke^{-rt_k}$. These boundary values are each interpolated by one hat function with the corresponding coefficients $u_{h,\,0}^{k=0,1,\ldots,\,N_t}$ and $u_{h,\,i=1,\ldots,\,N_s}^{0}$. This means these coefficients are known and we only have N_s unknown coefficients left. Hence, we may cancel the first column and row of matrix $M^{LQ}+\frac{\triangle t_k}{2}A^{LQ}$, the first row of matrix $(M^{LQ}-\frac{\triangle t_k}{2}A^{LQ})\,u_h^{k-1}$ and the first element of vectors u_h^k. The matrix $(M^{LQ}+\frac{\triangle t_k}{2}A^{LQ})$ then has size $N_s\times N_s$ and $(M^{LQ}-\frac{\triangle t_k}{2}A^{LQ})u_h^{k-1}$ then has dimension $N_s\times 1$ and vector u_h^k now has size $N_s\times 1$. The boundary terms that were dropped during this reduction process are put into a vector c^k with sizes $N_s\times 1$, and the final system of equations will have the following form:

$$(M^{LQ}+\frac{\triangle t_k}{2}A^{LQ})u_h^k=(M^{LQ}-\frac{\triangle t_k}{2}A^{LQ})u_h^{k-1}-c^k \tag{72}$$

in which $c^k=\begin{pmatrix}(m_{1,0}^{LQ}+\frac{\triangle t_k}{2}a_{1,0}^{LQ})\,u_{h,\,0}^k\\0\\...\\0\\0\end{pmatrix}$ and $u_h^k=\begin{pmatrix}u_{h,\,1}^k\\u_{h,\,2}^k\\...\\u_{h,\,N_s-1}^k\\u_{h,\,N_s}^k\end{pmatrix}$.

The linear system of equations (**72**) is equivalent to one with homogeneous boundary conditions, where the function vanishes on the boundary. We can rewrite the linear system of equations (**72**) in the form

$E^{LQ}u_h^k=F^{LQ}u_h^{k-1}-c^k$, and the entries of matrices E^{LQ} and F^{LQ} are below, respectively

$$e_{i,\,i}^{LQ}=(\frac{-rs_{i-1}\rho_{i-1}}{2}+\frac{h_i}{3})+(\frac{rs_{i+1}\rho_i}{2}+\frac{h_{i+1}}{3})$$

$$+\frac{\triangle t_k}{2}(s_{i+1}\rho_i r^2+s_i r^2\frac{\rho_i s_{i+1}}{h_{i+1}})$$

$$+\frac{\triangle t_k}{2}(s_i r^2 \frac{\rho_{i-1} s_{i-1}}{h_i} - r^2 s_{i-1}\rho_{i-1})$$

$$+\frac{\triangle t_k}{2}\frac{s_i^{2(\gamma+1)}\sigma_0^2}{2}(\frac{1}{h_i}+\frac{1}{h_{i+1}})$$

$$+\frac{\triangle t_k}{2}\frac{r(h_i+h_{i+1})}{2}, \quad 1 \le i \le N_s - 1$$

$$e^{LQ}_{i,\,i-1} = \frac{h_i}{6} - \frac{\rho_{i-1}s_{i-1}r}{2} - \frac{\triangle t_k}{2}\frac{\rho_{i-1}r^2 s_i s_{i-1}}{h_i}$$

$$+\frac{\triangle t_k}{2}(-\frac{\sigma_0^2 s_i^{2(\gamma+1)}}{2h_i} + \frac{r s_i}{2}),\ 2 \le i \le N_s$$

$$e^{LQ}_{i,\,i+1} = \frac{h_{i+1}}{6} + \frac{\rho_i s_{i+1} r}{2} + \frac{\triangle t_k}{2}\frac{\rho_i r^2 s_i s_{i+1}}{h_{i+1}}$$

$$+\frac{\triangle t_k}{2}(\frac{s_i^{2(\gamma+1)}\sigma_0^2}{2h_{i+1}} + \frac{r s_i}{2}),\ 1 \le i \le N_s - 1$$

$$e^{LQ}_{N_s,\,N_s} = \frac{\triangle t_k}{2}\frac{\rho_{N_s-1}r^2 s_{N_s}s_{N_s-1}}{h_{N_s}}$$

$$+\frac{\triangle t_k}{2}(\frac{s_{N_s}^{2(\gamma+1)}\sigma_0^2}{2h_{N_s}} - \frac{r s_{N_s-1}}{2})$$

$$-\frac{\triangle t_k}{2}r^2\rho_{N_s-1}s_{N_s-1}$$

$$+\frac{h_{N_s}}{3} - \frac{\rho_{N_s-1}r s_{N_s-1}}{2}$$

$$f^{LQ}_{i,\,i} = (\frac{-r s_{i-1}\rho_{i-1}}{2} + \frac{h_i}{3}) + (\frac{r s_{i+1}\rho_i}{2} + \frac{h_{i+1}}{3})$$

$$-\frac{\triangle t_k}{2}(s_{i+1}\rho_i r^2 + s_i r^2 \frac{\rho_i s_{i+1}}{h_{i+1}})$$

$$- \frac{\triangle t_k}{2}(s_i r^2 \frac{\rho_{i-1} s_{i-1}}{h_i} - r^2 s_{i-1}\rho_{i-1})$$

$$- \frac{\triangle t_k}{2}\frac{s_i^{2(\gamma+1)}\sigma_0^2}{2}(\frac{1}{h_i} + \frac{1}{h_{i+1}})$$

$$- \frac{\triangle t_k}{2}\frac{r(h_i + h_{i+1})}{2}, \quad 1 \le i \le N_s - 1$$

$$f^{LQ}_{i,\,i-1} = \frac{h_i}{6} - \frac{\rho_{i-1} s_{i-1} r}{2} - \frac{\triangle t_k r s_i}{4} + \frac{\triangle t_k}{2}\frac{\rho_{i-1} r^2 s_i s_{i-1}}{h_i}$$

$$- \frac{\triangle t_k}{2}(-\frac{\sigma_0^2 s_i^{2(\gamma+1)}}{2h_i}), \; 2 \le i \le N_s$$

$$f^{LQ}_{i,\,i+1} = \frac{h_{i+1}}{6} + \frac{\rho_i s_{i+1} r}{2} - \frac{\triangle t_k}{2}\frac{\rho_i r^2 s_i s_{i+1}}{h_{i+1}}$$

$$+ \frac{\triangle t_k r s_i}{4} - \frac{\triangle t_k s_i^{2(\gamma+1)}\sigma_0^2}{4h_{i+1}}, \; 1 \le i \le N_s - 1$$

$$f^{LQ}_{N_s,\,N_s} = \frac{-\triangle t_k}{2}\frac{\rho_{N_s-1} r^2 s_{N_s} s_{N_s-1}}{h_{N_s}}$$

$$- \frac{\triangle t_k}{2}(\frac{s_{N_s}^{2(\gamma+1)}\sigma_0^2}{2h_{N_s}} - \frac{r s_{N_s-1}}{2})$$

$$+ \frac{\triangle t_k}{2} r^2 \rho_{N_s-1} s_{N_s-1}$$

$$+ \frac{h_{N_s}}{3} - \frac{\rho_{N_s-1} r s_{N_s-1}}{2}$$

With these formulas and the given value of $u_h^0 = max(K - s, 0)$, we compute iteratively the unknown variables $u_{h,\,i}^k$ for $i = 1, 2, \ldots, N_s$, and $k = 1, 2, \ldots, N_t$, and obtain the prices of our put option for any given values of both time $t \in [0,\, 1]$ and the underlying asset $s \in [0,\, S_b]$.

For option 2's formulation with Crank-Nicolson scheme, using exactly the same calculations as in option 1, the entries for the mass and stiffness matrix M and A are

$$m^{LQ}_{i,\,i-1} = \frac{h_i}{6} \; - \; \frac{p_{i-1} r}{6}(s_i + 2s_{i-1}), \;\; 1 \leq i \leq N_s$$

$$m^{LQ}_{i,\,i} = (\frac{-r s_{i-1} \rho_{i-1}}{2} + \frac{h_i}{3}) + \frac{r s_{i+1} \rho_i}{2}$$

$$+ \frac{h_{i+1}}{3}, \;\; 1 \leq i \leq N_s - 1$$

$$m^{LQ}_{0,\,0} = \frac{h_1}{3} \; - \; \frac{\rho_0 r h_1}{6}$$

$$m^{LQ}_{N_s,\,N_s} = \frac{h_{N_s}}{3} \; + \; \rho_{N_s - 1} r (\frac{s_{N_s - 1}}{6} + \frac{s_{N_s}}{3})$$

$$m^{LQ}_{i,\,i+1} = \frac{h_{i+1}}{6} \; + \; \frac{\rho_i r}{6}(s_i + 2s_{i+1}), \;\; 0 \leq i \leq N_s - 1$$

$$a^{LQ}_{i,\,i-1} = - \frac{\sigma_0^2 s_i^{2(\gamma+1)}}{2h_i} \; + \; \frac{r s_i}{2}, \;\; 1 \leq i \leq N_s$$

$$a^{LQ}_{i,\,i+1} = - \frac{s_i^{2(\gamma+1)} \sigma_0^2}{2h_{i+1}} \; - \; \frac{r s_i}{2}, \;\; \; 0 \leq i \leq N_s - 1$$

$$a^{LQ}_{0,0} = \frac{r s_1}{2}$$

$$a^{LQ}_{N_s,\,N_s} = \frac{s_{N_s}^{2(\gamma+1)} \sigma_0^2}{2h_{N_s}} \; - \; \frac{r s_{N_s - 1}}{2}$$

$$a^{LQ}_{i,\,i} = \frac{s_i^{2(\gamma+1)} \sigma_0^2}{2}(\frac{1}{h_i} + \frac{1}{h_{i+1}}) + \frac{r(h_i + h_{i+1})}{2}, \;\; 1 \leq i \leq N_s - 1$$

2.5 Mesh Refinements

For improving the accuracy of our numerical solutions to the equation (**14**) with boundary conditions (**15**) − (**16**), especially when s is near the strike price $K = 50$ and S_b, we extend the mesh in the S-direction (that is, add another interval $[S_b, S_\infty]$, where S_∞ is a very large number, $30K$) and divide the new interval $[0, S_\infty]$ into three subintervals $[0, K]$, $[K, S_b]$ and $[S_b, S_\infty]$. Then we discretize each of the subintervals as follows: First, we use either the same uniform partition or geometric partition, which was described at the beginning of Section (3.4), with N_1 and N_2 subintervals for $[0, K]$ and $[K, S_b]$, respectively. Second, we decide to employ the geometric partition for the interval $[S_b, S_\infty]$ with N_3 subintervals $h_{N_2+N_1+1}$, $h_{N_2+N_1+2}$,..., $h_{N_3+N_2+N_1}$ followed by the similar geometric partition used for $[K, S_b]$ but now the geometric ratio r_3 is determined by the equation $h_{N_2+N_1+1} = {r_3}^{N_3-1} h_{N_3+N_2+N_1} = h_{N_3+N_2+N_1}^{\frac{1+\gamma}{2}}$. Our discrete space $V_h^b \in H_0^1([0, S_b])$ now becomes $V_h^\infty \in H_0^1([0, S_\infty])$.

The reason we choose $h_{N_3+N_2+N_1}^{max(\frac{1}{2}, \frac{1+\gamma}{2})}$ can be explained as follows: we pick u in equation (**22**) as a function that will decay quickly when $s \to \infty$, such as $u = \frac{1}{s^c}$ for some parameters c. Let $\varphi = u$, we want to find the best constant c such that each of the following integral in equation (22) converges:

$$(\alpha \frac{\partial \varphi}{\partial s}, \frac{\partial \varphi}{\partial s}) = \frac{-c(c+1)}{2} \int_0^\infty s^{2\gamma-2c} ds = \frac{-c(c+1)}{2} \frac{s^{2\gamma-2c+1}}{2\gamma-2c} |_0^\infty$$

$$\text{converges only when } c \geq \frac{1+\gamma}{2}$$

$$(\beta \frac{\partial \varphi}{\partial s}, \varphi) = \int_0^\infty \frac{[(1+\gamma)\sigma_0^2 s^{2\gamma+1} - rs]}{s^{2c+1}} ds$$

$$= (1+\gamma)\sigma_0^2 s^{2(\gamma-c)+1} - \frac{r s^{-2c+1}}{-2c+1} |_0^\infty$$

$$\text{converges only when } c \geq max(\frac{1}{2}, \frac{1+\gamma}{2})$$

$$(r\varphi,\, \varphi) = r\int_0^\infty \frac{1}{s^{2c}}ds \;= \frac{rs^{-2c+1}}{-2c+1}|_0^\infty ds \quad \text{converges only when } c \geq \frac{1}{2}$$

Therefore, since $\gamma > -1$, we need to choose $c = max(\frac{1+\gamma}{2},\, \frac{1}{2})$ since the convergence rate of our error will decay slower than $h_{N_3+N_2+N_1}^{max(\frac{1}{2},\frac{1+\gamma}{2})}$. Now we can find the unique pair $(r_3,\, N_3)$ in the same way used to find the pair $(r_1,\, N_1)$, and the formula is

$$(r_3,\, N_3) \;=$$

$$(\frac{S_\infty - S_b - h_{N_3+N_2+N_1}}{S_\infty - S_b - (h_{N_3+N_2+N_1})^{max(\frac{1}{2},\,\frac{1+\gamma}{2})}}\,, (max(\frac{1}{2}\,, \frac{1+\gamma}{2}) - 1)\frac{log\, h_{N_3+N_2+N_1}}{log\, r_3} \;+ 1)$$

Combining the new geometric partition for $[S_b,\, S_\infty]$ with the uniform partition or geometric partition for each of the subinterval $[0,\, K]$ and $[K,\, S_b]$, we have four options to choose for discretizations in the S-direction.

We employ a non-equidistant partition only in the S-direction, since having a mesh with an uniform parition in the T-direction gives the most accurate numerical solutions, especially when the local volatility is sufficiently large ($\geq$ 0.7). Our purpose for discretizing the S-direction nonuniformly is to increase the number of points near the point $u(K,\, 0)$ and $u(S_b,\, 1)$. This method helps eliminate the errors when the underlying asset price is near S_b. Therefore, this non-equidistant mesh gives a much better accuracy, even for the cases when the local volatility is very high (that is, when $\sigma \geq 0.8$). However, the trade-off is that this mesh requires a large number of points, and the required time of calculation increases proportionally for higher fineness of the mesh (increase value of either N_1,N_2 or N_3).

3 Numerical results

A feature of the FEM method when applying it to solve the PDE representation of option pricing is the knowledge about the development of the option value function for each time step, which is definied as the complete term structure of the option. We can easily visualize the whole term structure of the European put option as in Figure 3 below. At the present time, $t = 0$, which is the "front edge" of the surface, one can clearly see the shape of the

non-smooth payoff function $u(s,\,0) = (K - s)^+$. By solving the functions $u(s,\,t)$ for each s over the life-time of the option (that is, for each t runs from 0 to 1), the complete term structure is obtained. Towards the maturity time, $t = 1$, after N_t time steps, we approach the function $u(s,\,1)$. Of the whole option surface, the special points of interest are near the points $u(K,\,0)$ and $u(S_b,\,1)$ in which the errors of our numerical solutions were mainly distributed.

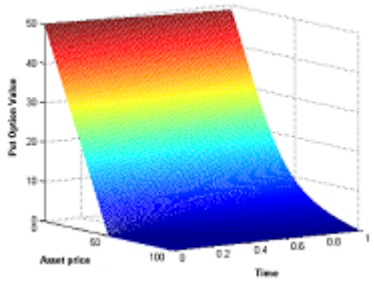

Figure 3: Values of a put option with $S_b = 100$, $K = 50$, $\sigma = 0.5$, $r = 0.03$, $N_t = 200$, $N_s = 1000$, $S_\infty = 1500$, $N_3 = 1000$, geometric partition in S and uniform partition in T

We set our parameters as follows: $K = 50$, $\gamma = 0$, $S_b = 2K$, $r = 0.03$, $N_t = 200$, $N_s = 1000$,$T = 1$, $S_\infty = 30K$, $N_3 = 1000$. We will run our numerical schemes in two cases with $\sigma = 0.4$ and $\sigma = 0.8$. For each of these cases, we use either the uniform partitions for the interval $[0,\,S_b]$ or extend the mesh by adding another interval $[S_b,\,S_\infty]$ and for the new interval $[0,\,S_\infty]$, the geometric partition described in Section 4.5 is applied for $[S_b,\,S_\infty]$ and the same uniform partition for $[0,\,S_b]$. In addition, for the T-direction, we employ the uniform partition in $[0,\,T]$. For the two mesh refinements, define a domain $\mathrm{D} = [0,\,T] \times [0,\,S_b]$ and compute the L^2(D)- norm and L^∞(D)-norm errors (see Table 1) when comparing our numerical solutions to the exact solutions $f(s,\,t)$ given the Black-Scholes formula, and compute the reduction factors of our errors in each case. The formulas for the L^2(D)-norm and L^∞(D)- norm errrors are,

$$L^2(\mathrm{D})\text{-norm error} =$$

$$[\sum_{i,\,j=0}^{i=N_s-1,\,j=N_t-1} (\frac{f(s_i,\,t_j) + f(s_{i+1},\,t_j) + f(s_i,\,t_{j+1}) + f(s_{i+1},\,t_{j+1})}{4}$$

$$-\frac{u(s_i,\, t_j) + u(s_{i+1},\, t_j) + u(s_i,\, t_{j+1}) + u(s_{i+1},\, t_{j+1})}{4})^2$$

$$\times(t_{j+1} - t_j)(s_{i+1} - s_i)]^{\frac{1}{2}} \tag{73}$$

$$L^\infty(\mathrm{D})\text{-norm error} = max_{1\le i\le N_s,\, 1\le j\le N_t}|u(s_i,\, t_j) - f(s_i,\, t_j)| \tag{74}$$

Based on the errors, we determine if adding the new interval $[S_b,\, S_\infty]$ with geometric partition improves the accuracy of our numerical solutions. Figures 4 - 7 are the graphs of the errors for each mesh refinement when $\sigma = 0.4$ and $\sigma = 0.8$. The exact solutions $f(s,\, t)$ for these two cases given by the Black-Scholes formula are also shown in Figures 8 - 9. Since the investor mainly concerns about the errors of our numerical solutions at time $t = 1$, define a domain $\Omega = [T] \times [0,\, S_b]$, the $L^2(\Omega)$- norm and $L^\infty(\Omega)$- norm of those errors and the reduction factors are also shown in Table 2 for cases when $\sigma = 0.4$. The formulas for the errors in $L^2(\Omega)$- norm and $L^\infty(\Omega)$- norm at time $t = 1$ are:

$$L^2(\Omega)\text{-norm error at time } 1 =$$

$$[\sum_{i=0}^{i=N_s-1}(\frac{f(s_{i+1},\, t_{N_t}) + f(s_i,\, t_{N_t}) - u(s_{i+1},\, t_{N_t}) - u(s_i,\, t_{N_t})}{2})^2$$

$$\times(s_{i+1} - s_i)]^{\frac{1}{2}} \tag{75}$$

$$L^\infty(\Omega)\text{-norm error at time } 1 = max_{1\le i\le N_s}|u(s_i,\, t_{N_t}) - f(s_i,\, t_{N_t})| \tag{76}$$

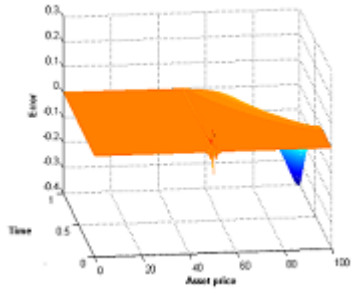

Figure 4: Errors by uniform partition in [0, 100] and in T with $K = 50$, $\gamma = 0$, $S_b = 100$, $r = 0.03$, $N_t = 200$, $N_s = 1000$, $T = 1$, $S_\infty = 1500$, $N_3 = 1000$, $\sigma = 0.4$

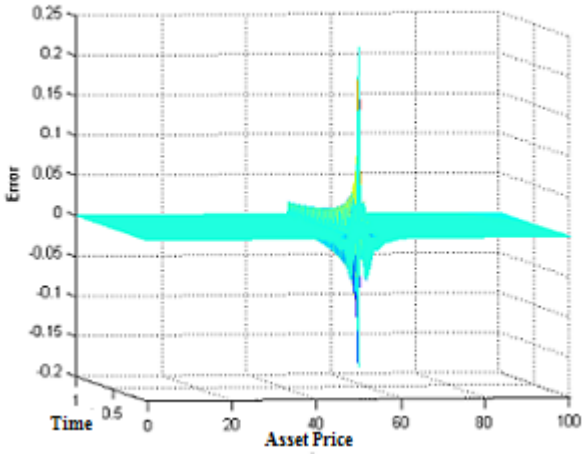

Figure 5: Errors by uniform partition in [0, 100] and geometric partition in [100, 1500], uniform partition in T with $K = 50$, $\gamma = 0$, $S_b = 100$, $r = 0.03$, $N_t = 200$, $N_s = 1000$, $T = 1$, $S_\infty = 1500$, $N_3 = 1000$, $\sigma = 0.4$

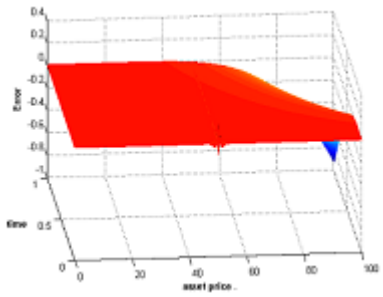

Figure 6: Errors by uniform partition in [0, 100] and in T with $K = 50$, $\gamma = 0$, $S_b = 100$, $r = 0.03$, $N_t = 200$, $N_s = 1000$, $T = 1$, $S_\infty = 1500$, $N_3 = 1000$, $\sigma = 0.8$

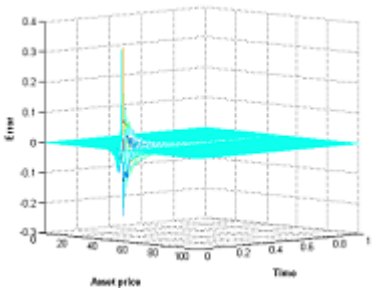

Figure 7: Errors by uniform partition in [0, 100] and geometric partition in [100, 1500], uniform partition in T with $K = 50$, $\gamma = 0$, $S_b = 100$, $r = 0.03$, $N_t = 200$, $N_s = 1000$, $T = 1$, $S_\infty = 1500$, $N_3 = 1000$, $\sigma = 0.8$

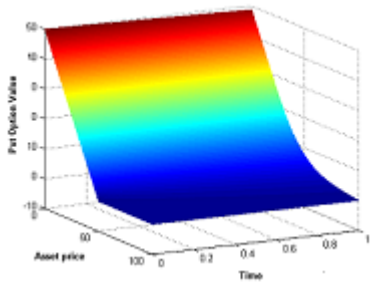

Figure 8: Solutions by Black-Scholes formula with $K = 50$, $\gamma = 0$, $r = 0.03$, $T = 1$, $\sigma = 0.4$, $N_t = 200$, $N_s = 1000$, $S_\infty = 1500$, $N_3 = 1000$

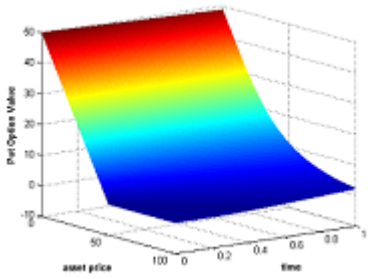

Figure 9: Solutions by Black-Scholes formula with $K = 50$, $\gamma = 0$, $r = 0.03$, $T = 1$, $\sigma = 0.8$, $N_t = 200$, $N_s = 1000$,$S_\infty = 1500$, $N_3 = 1000$

Type of partition	L^2(D)-norm error ($\sigma = 0.4$)	L^2(D)-norm error ($\sigma = 0.8$)	L^∞(D)-norm error ($\sigma = 0.4$)	L^∞(D)-norm error ($\sigma = 0.8$)
Uniform partition in [0,100]	0.2182	0.2725	0.4091	0.8259
Geometric partition in [100,1500]	0.0515	0.0537	0.2016	0.2826
Reduction Factor	4.24	5.07	2.03	3.02

Table 1: L^2(D)- norm and L^∞(D)- norm errors when $\sigma = 0.4$ and $\sigma = 0.8$ with $K = 50$, $\gamma = 0$, $S_b = 100$, $r = 0.03$, $N_t = 200$, $N_s = 1000$, $T = 1$, $S_\infty = 30K$, $N_3 = 1000$

Type of partition	$L^2(\Omega)$-norm error ($\sigma = 0.4$)	$L^2(\Omega)$-norm error ($\sigma = 0.8$)	$L^\infty(\Omega)$-norm error ($\sigma = 0.4$)	$L^\infty(\Omega)$-norm error ($\sigma = 0.8$)
Uniform partition in [0,100]	0.1455	0.1696	0.3942	0.7827
Geometric partition in [100,1500]	0.0078	0.0051	0.028	0.0474
Reduction Factor	18.65	33.25	14.08	16.51

Table 2: $L^2(\Omega)$- norm and $L^\infty(\Omega)$- norm errors when $\sigma = 0.4$ and $\sigma = 0.8$ with $K = 50$, $\gamma = 0$, $S_b = 100$, $r = 0.03$, $N_t = 200$, $N_s = 1000$, $S_\infty = 30K$, $N_3 = 1000$

Looking at Figures $4 - 7$ and Table 1 above, we see that by adding the new interval $[S_b, S_\infty]$ with geometric partition in the S- direction, the major errors near the point $u(S_b, 1)$ are eliminated, although the errors near the point $u(K, 0)$ slightly increase. However, by using an extended mesh refinement on $[0, S_\infty]$, the errors in L^2(D)- norm and L^∞(D)- norm are reduced by a factor larger than 2 compared to the errors obtained when using only the

mesh $[0,\ S_b]$. The reduction factors of those errors at time $t = 1$ are quite significant (greater than 14, see Table 2), which shows the advantage of an extended mesh refinement by eliminating most of the errors at that time. In general, this extended mesh refinement indeed helps improve the accuracy of our numerical solutons. Therefore, from this point, we will always include the new interval $[S_b,\ S_\infty]$ with geometric partition when doing the refinement in the S- direction.

We also run our numerical schemes when $S_b = 1.2K$ (that is, using less number of points in the S-direction), but the result is not sufficiently good.

With the same set of parameters $K = 50$, $\gamma = 0$, $S_b = 2K$, $r = 0.03$, $\sigma = 0.4$, $S_\infty = 30K$, $N_3 = 1000$, we now compare the errors in L^2(D)-norm and L^∞(D)- norm (formulas (73) and (74)) when using different partitions for the intervals $[0,\ S_b]$ and $[0,\ T]$ with different number of subintervals N_s and N_t to determine which partition best improves the accuracy of our numerical solutions. Note that we always use the geometric partition for $[S_b,\ S_\infty]$ because it helps eliminate the major errors near the points $u(S_b,\ 1)$. There are exactly four possibilities of partitions in $[0,\ S_b] \times [0,\ T]$: geometric partition for $[0,\ S_b]$ and uniform partition for $[0,\ T]$, uniform partition for $[0,\ S_b]$ and geometric partition for $[0,\ T]$, uniform partition for $[0,\ S_b]$ and uniform partition for $[0,\ t]$, geometric partition for $[0,\ S_b]$ and geometric partition for $[0,\ T]$. However, we tried our numerical schemes using uniform partition for $[0,\ S_b]$ and geometric partition for $[0,\ T]$ and got bad results. We also computed the reduction factor of our errors in L^2(D)- norm and L^∞(D)-norm for each of the other three refinements to determine the approximated convergence rate of our reduction factor. The complete details are shown in Tables 3 - 5 below. Since the investor mainly concerns about the errors of our numerical solutions at time $t = 1$, the $L^2(\Omega)$- norm and $L^\infty(\Omega)$- norm of our errors and the reduction factors are also shown in Tables 6 - 8 for cases when $\sigma = 0.4$.

$(N_s,\ N_t)$	Max $h_{i=1,\ldots,N_s}$, max $\Delta t_{j=1,\ldots,N_t}$	Min $h_{i=1,\ldots,N_s}$, min $\Delta t_{j=1,\ldots,N_t}$	L^2(D)-norm error ($\sigma = 0.4$)	L^∞(D)-norm error ($\sigma = 0.4$)	Reduction Factor in L^2(D)-norm	Reduction Factor in L^∞(D)-norm
(2000,400)	0.05, 0.0025	0.05, 0.0025	0.028	0.1376		
(1000,200)	0.1, 0.005	0.1, 0.005	0.0515	0.2106	1.84	1.53
(500,100)	0.2, 0.01	0.2, 0.01	0.0901	0.3053	1.75	1.45
(250,50)	0.4, 0.02	0.4, 0.02	0.1462	0.4030	1.62	1.32

Table 3: L^2(D)- norm and L^∞(D)- norm errors for uniform partitions in both $S - T$ directions with $K = 50$, $\gamma = 0$, $S_b = 100$, $r = 0.03$, $\sigma = 0.4$, $T = 1$, $S_\infty = 1500$, $N_3 = 1000$

(N_s, N_t)	Max $h_{i=1,...,N_s}$, max $\Delta t_{j=1,...,N_t}$	Min $h_{i=1,...,N_s}$, min $\Delta t_{j=1,...,N_t}$	L^2(D)-norm error ($\sigma = 0.4$)	L^∞(D)-norm error ($\sigma = 0.4$)	Reduction Factor in L^2(D)-norm	Reduction Factor in L^∞(D)-norm
(2000,400)	0.1090, 0.00125	0.0094, 0.00125	0.0016	0.0688		
(1000,200)	0.1830, 0.005	0.0231, 0.005	0.0058	0.1397	3.63	2.03
(500,100)	0.35, 0.01	0.0515, 0.01	0.0149	0.1948	2.57	1.39
(250,50)	0.4527, 0.02	0.1544, 0.02	0.0185	0.2632	1.24	1.35

Table 4: L^2(D)- norm and L^∞(D)- norm errors for geometric partition in S, uniform partition in T with $K = 50$, $\gamma = 0$, $S_b = 100$, $r = 0.03$, $\sigma = 0.4$, $T = 1$, $S_\infty = 1500$, $N_3 = 1000$

(N_s, N_t)	Max $h_{i=1,...,N_s}$, max $\Delta t_{j=1,...,N_t}$	Min $h_{i=1,...,N_s}$, min $\Delta t_{j=1,...,N_t}$	L^2(D)-norm error ($\sigma = 0.4$)	L^∞(D)-norm error ($\sigma = 0.4$)	Reduction Factor in L^2(D)-norm	Reduction Factor in L^∞(D)-norm
(2000,400)	0.1090, 0.0106	0.0094, 0.0000038	0.0029	0.0856		
(1000,200)	0.2230, 0.0144	0.0231, 0.00009	0.0076	0.1413	2.62	1.65
(500,100)	0.35, 0.0228	0.0515, 0.00005	0.0172	0.1983	2.26	1.40
(250,50)	0.4527, 0.0416	0.1544, 0.0006	0.0289	0.2747	1.68	1.39

Table 5: L^2(D)- norm and L^∞(D)- norm errors for geometric partition in both S-T directions with $K = 50$, $\gamma = 0$, $S_b = 100$, $r = 0.03$, $\sigma = 0.4$, $T = 1$, $S_\infty = 1500$, $N_3 = 1000$

(N_s, N_t)	$L^2(\Omega)$-norm error ($\sigma = 0.4$)	$L^\infty(\Omega)$-norm error ($\sigma = 0.4$)	Reduction Factor in $L^2(\Omega)$-norm	Reduction Factor in $L^\infty(\Omega)$-norm
(2000,400)	0.0033	0.0195		
(1000,200)	0.0078	0.028	2.36	1.43
(500,100)	0.0174	0.039	2.23	1.39
(250,50)	0.0341	0.048	1.96	1.33

Table 6: $L^2(\Omega)$- norm and $L^\infty(\Omega)$- norm errors for uniform partition in both $S - T$ directions with $K = 50$, $\gamma = 0$, $S_b = 100$, $r = 0.03$, $\sigma = 0.4$, $T = 1$, $S_\infty = 1500$, $N_3 = 1000$

(N_s, N_t)	$L^2(\Omega)$-norm error ($\sigma = 0.4$)	$L^\infty(\Omega)$-norm error at t = 1 ($\sigma = 0.4$)	Reduction Factor in $L^2(\Omega)$-norm	Reduction Factor in $L^\infty(\Omega)$-norm
(2000,400)	0.00038	0.0014		
(1000,200)	0.0012	0.0031	3.16	2.24
(500,100)	0.0043	0.0045	3.07	1.45
(250,50)	0.0127	0.0067	2.95	1.49

Table 7: $L^2(\Omega)$- norm and $L^\infty(\Omega)$- norm errors for geometric partition in S, uniform partition in T with $K = 50$, $\gamma = 0$, $S_b = 100$, $r = 0.03$, $\sigma = 0.4$, $S_\infty = 1500$, $N_3 = 1000$

(N_s, N_t)	$L^2(\Omega)$-norm error ($\sigma = 0.4$)	$L^\infty(\Omega)$-norm error ($\sigma = 0.4$)	Reduction Factor in $L^2(\Omega)$-norm	Reduction Factor in $L^\infty(\Omega)$-norm
(2000,400)	0.00067	0.0018		
(1000,200)	0.0019	0.0052	2.83	2.89
(500,100)	0.0052	0.0145	2.88	2.79
(250,50)	0.0143	0.0288	2.76	1.81

Table 8: $L^2(\Omega)$- norm and $L^\infty(\Omega)$- norm errors for geometric partition in both S-T directions with $K = 50$, $\gamma = 0$, $S_b = 100$, $r = 0.03$, $\sigma = 0.4$, $S_\infty = 1500$, $N_3 = 1000$

From Tables 3 - 8, we find that for sufficiently large values of N_s and N_t, the geometric partition in S and uniform partition in T for the intervals $[0, S_b]$ and $[0, T]$ gives the smallest L^2(D)- norm and L^∞(D)- norm errors and the highest reduction factors in both L^2(D)-norm and L^∞(D)-norm. The approximated rate of convergence for each type of partition, in the order above, is: 1.84, 3.63, 2.62 in L^2(D)-norm and 1.53, 2.53, 1.65 in L^∞(D)-norm. At time $t = 1$, such rate of convergence in the same order is: 2.36, 3.16, 2.83 in $L^2(\Omega)$-norm and 1.43, 2.24, 2.89 in $L^\infty(\Omega)$-norm. Due to these results, we determine to use the geometric partition in S and uniform partition in T for the interval $[0, S_b]$ for all the following tests, since out of the four partitions, that partition improves the accuracy of our solutions the most.

Although the geometric partition in S, uniform partition in T for the interval $[0, S_b] \times [0, T]$ and geometric partition for $[S_b, S_\infty]$ is a good choice, we realize that for sufficiently large σ (that is, $\sigma \geq 0.7$), our numerical schemes can reduce the errors near the point $u(K, 0)$ by applying the Galerkin Least Square (GLS) stabilization method presented in Section 4.4. With the same set of parameters $K = 50$,$\gamma = 0$, $S_b = 2K$, $r = 0.03$,$N_t = 200$, $N_s = 1000$, $S_\infty = 30K$, $N_3 = 1000$, we run our numerical schemes with GLS and the classical FEM for wo cases when $\sigma = 0.4$ (sufficiently small value) and $\sigma = 0.8$ (sufficiently large value). The errors of our numerical solutions are shown in Figure 10 - 14. We also compute the L^2(D)- norm and L^∞(D)- norm errors using formulas (73) and (74) to see the advantage of applying the GLS (see Table 9). The errors in $L^2(\Omega)$-norm and $L^\infty(\Omega)$-norm at time $t = 1$, which was the main concern of investors, are also shown in Table 10 for two cases of $\sigma = 0.4$ and 0.8.

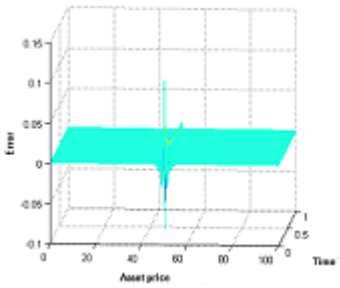

Figure 10: Errors with GLS when $K = 50$, $\gamma = 0$, $S_b = 100$, $r = 0.03$, $N_t = 200$, $N_s = 1000$, $S_\infty = 1500$, $N_3 = 1000$, $\sigma = 0.4$, geometric partition in S and uniform partition in T

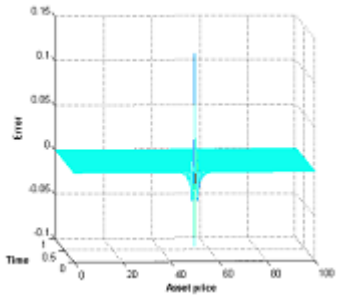

Figure 11: Errors with classical FEM when $K = 50$, $\gamma = 0$, $S_b = 100$, $r = 0.03$, $N_t = 200$, $N_s = 1000$, $S_\infty = 1500$, $N_3 = 1000$, $\sigma = 0.4$, geometric partition in S and uniform partition in T

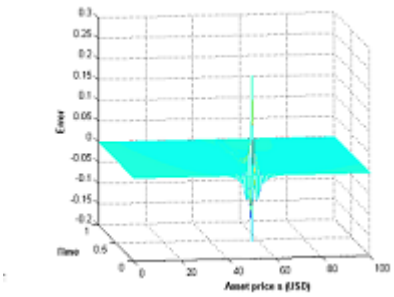

Figure 12: Errors with GLS when $K = 50$, $\gamma = 0$, $S_b = 100$, $r = 0.03$, $N_t = 200$, $N_s = 1000$, $S_\infty = 1500$, $N_3 = 1000$, $\sigma = 0.8$, geometric partition in S and uniform partition in T

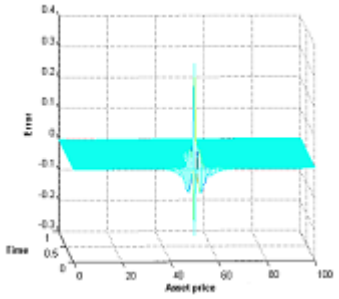

Figure 13: Errors with classical FEM when $K = 50$, $\gamma = 0$, $S_b = 100$, $r = 0.03$, $N_t = 200$, $N_s = 1000$, $S_\infty = 1500$, $N_3 = 1000$, $\sigma = 0.8$, geometric partition in S and uniform partition in T

Numerical scheme	L^2(D)-norm error ($\sigma = 0.4$)	L^∞(D)-norm error ($\sigma = 0.4$)	L^2(D)-norm error ($\sigma = 0.8$)	L^∞(D)-norm error ($\sigma = 0.8$)
Classical FEM	0.0058	0.1197	0.0162	0.2634
GLS	0.0021	0.0644	0.0083	0.1488
Reduction factor	2.76	1.86	1.95	1.77

Table 9: L^2(D)- norm and L^∞(D)- norm errors for $\sigma = 0.4$ and $\sigma = 0.8$ with $K = 50$, $\gamma = 0$, $S_b = 100$, $r = 0.03$, $N_t = 200$, $N_s = 1000$, $T = 1$, $S_\infty = 1500$, $N_3 = 1000$, geometric partition in S and uniform partition in T

Numerical scheme	$L^2(\Omega)$-norm error($\sigma = 0.4$)	$L^\infty(\Omega)$-norm error ($\sigma = 0.4$)	$L^2(\Omega)$-norm error ($\sigma = 0.8$)	$L^\infty(\Omega)$-norm error ($\sigma = 0.8$)
Classical FEM	0.0012	0.0031	0.0085	0.0157
GLS	0.0005	0.0017	0.0044	0.0096
Reduction factor	2.4	1.82	1.92	1.64

Table 10: $L^2(\Omega)$- norm and $L^\infty(\Omega)$- norm errors for $\sigma = 0.4$ and $\sigma = 0.8$ with $K = 50$, $\gamma = 0$, $S_b = 100$, $r = 0.03$, $N_t = 200$, $N_s = 1000$, $S_\infty = 1500$, $N_3 = 1000$, geometric partition in S and uniform partition in T

As we can see from Table 9 and 10, the GLS did a great job in reducing the errors near the singular point $u(K, 0)$. The reduction factors of our L^2(D)-norm and L^∞(D)- norm errors are almost as large as 2 and 1.8 even when σ is sufficient large (0.8), which is demonstrated in the real-world situations in which the option prices are highly volatile. At time $t = 1$, the reduction factors in $L^2(\Omega)$- norm and $L^\infty(\Omega)$- norm are a little bit smaller, 1.92 and 1.64. The feature of improving the accuracy of our numerical solutions even when σ is large is exactly the advantage of adding the GLS into our numerical schemes.

Finally, we consider applying the GLS on the same mesh refinements used in Figures 10 and 12 with the set of parameters $\sigma_0 = 0.3$, $K = 50$, $S_b = 2K$, $N_t = 200$, $N_s = 1000$, $r = 0.03$, $S_\infty = 30K$, $N_3 = 1000$ to run our numerical schemes in three scenarios: γ is negative ($\gamma = -0.03$), γ is positive ($\gamma = 0.07$) and $\gamma = 0$. We then obtain the numerical solutions for these three cases. Since there are no formulas to compute the exact solutions for $\gamma \neq 0$, we expect that our numerical solutions are approximately close to the correct solution, thus we compare our numerical solutions to those given by the Black-Scholes formula when $\gamma = 0$.

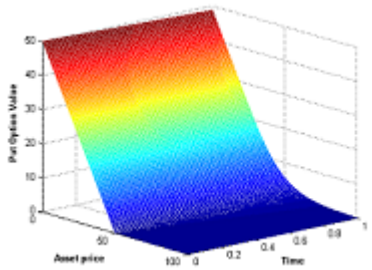

Figure 14: Numerical solutions in the case $\gamma = -0.03$, $S_\infty = 1500$, $N_3 = 1000$, $\sigma_0 = 0.3$, $K = 50$, $S_b = 100$, $N_t = 200$, $N_s = 1000$, $r = 0.03$, $T = 1$, geometric partition in S and uniform partition in T

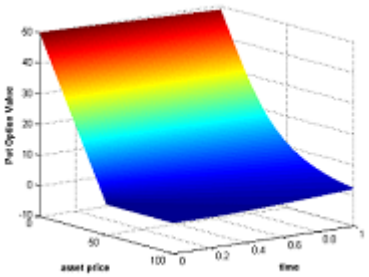

Figure 15: Solutions by Black-Scholes in the case $\gamma = 0$, $\sigma = 0.3$, $r = 0.03$, $T = 1$, $K = 50$, $S_b = 100$, $N_t = 200$, $N_s = 1000$, $S_\infty = 1500$, $N_3 = 1000$

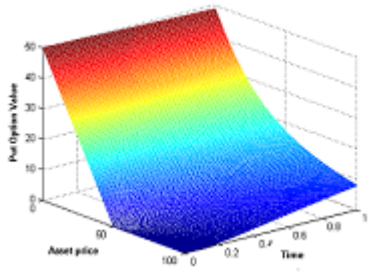

Figure 16: Numerical solutions in the case $\gamma = 0.07$, $S_\infty = 1500$, $N_3 = 1000$, $\sigma_0 = 0.3$, $K = 50$, $S_b = 2K$, $N_t = 200$, $N_s = 1000$, $r = 0.03$, $T = 1$, geometric partition in S and uniform partition in T

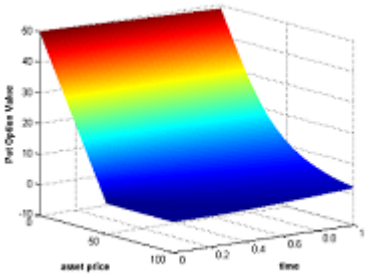

Figure 17: Solutions by Black-Scholes in the case $\gamma = 0$, $\sigma = 0.3$, $r = 0.03$, $T = 1$, $K = 50$, $S_b = 100$, $N_t = 200$, $N_s = 1000$, $S_\infty = 1500$, $N_3 = 1000$

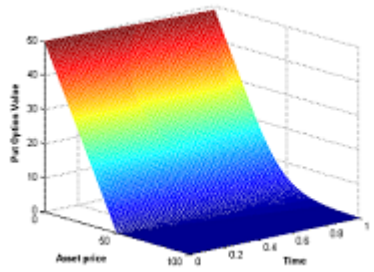

Figure 18: Numerical solutions in the case $\gamma = 0$, $S_\infty = 1500$, $N_3 = 1000$, $\sigma_0 = 0.3$, $K = 50$, $S_b = 2K$, $N_t = 200$, $N_s = 1000$, $r = 0.03$, $T = 1$, geometric partition in S and uniform partition in T

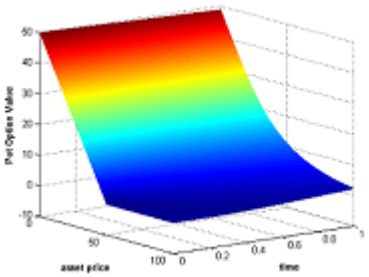

Figure 19: Solutions by Black-Scholes in the case $\gamma = 0$, $\sigma = 0.3$, $r = 0.03$, $T = 1$, $K = 50$, $S_b = 100$, $N_t = 200$, $N_s = 1000$, $S_\infty = 1500$, $N_3 = 1000$

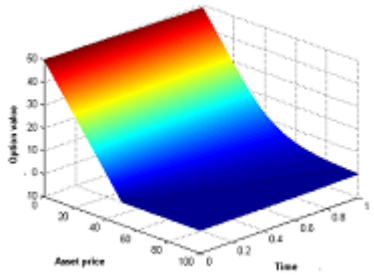

Figure 20: Numerical solutions in the case $\gamma = 0.07$, $S_\infty = 1500$, $N_3 = 2500$, $\sigma_0 = 0.3$, $K = 50$, $S_b = 100$, $N_t = 200$, $N_s = 1000$, $r = 0.03$, $T = 1$, geometric partition in S and uniform partition in T

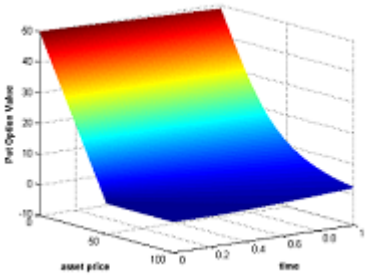

Figure 21: Solutions by Black-Scholes in the case $\gamma = 0$, $\sigma = 0.3$, $r = 0.03$, $T = 1$, $K = 50$, $S_b = 100$, $N_t = 200$, $N_s = 1000$, $S_\infty = 1500$, $N_3 = 1000$

Comparing the two pairs of figures side by side (Figures 14 -15 and Figures 18-19), we find that for the case when $\gamma = -0.3$ or $\gamma = 0$, the graph of our numerical solutions are very much similar to that of the exact solutions given by Black-Scholes formula. The L^2(D)- norm and L^∞(D)- norm errors, which were computed using formulas (73) - (74), when $\gamma = -0.3$, 0, 0.07 are 0.075, 0.0035, 1.4915 and 0.1461, 0.0019,1.2392, respectively. However,

when $\gamma = 0.07$, the graph of our numerical solutions are not similar to that of the exact solutions given by the Black-Scholes formula (see Figures 16 - 17), especially at the points near (100, 1), and the errors in L^2(D)-norm and L^∞(D)-norm are large (greater than 1). In such case, we improve the accuracy of our solutions by choosing N_3 to be a large number, such as $N_3 = 2500$, and obtain the graph of our numerical solutions very similar to that of the exact solutions (see Figures 20-21). Therefore, our numerical scheme may give a good approximation of the exact solutions for cases when $-0.3 \leq \gamma \leq 0$. Unfortunately, when γ is sufficiently positive ($\gamma \geq 0.07$), we need to increse significantly the number of subintervals (N_3) in the extended interval $[S_b, S_\infty]$ to achieve a sufficiently good approximation.

4 Conclusions

In this paper, we showed how to use the FEM to compute the numerical solutions of the PDE representation of an European put option pricing, including cases when the local volatility σ is not constant. We described such local volatility through the classic CEV model presented in Section 3. We also employ different mesh refinements, which help improve the accuracy of our numerical solutions. The most successful mesh refinement is an extended mesh $[0, S_\infty] \times [0, T]$ ($S_\infty$is chosen to be a very large number, $30K$) with geometric partition in the S direction and uniform partition in the T-direction. We computed the errors in L^2(D)- norm and L^∞(D)- norm and showed the high reduction factor of our errors when using such mesh refinement with large number of points in both S-T directions. Since the investor mainly concerns about the errors at time $t = 1$, we also computed our errors in $L^2(\Omega)$- norm and $L^\infty(\Omega)$- norm and obtained very good results. In addition, for cases when the option prices are highly volatile, which results in a large value of the local volatility $\sigma(\geq 0.7)$, we apply the GLS stabilization method on the same mesh refinement and achieve a sufficiently good approximation to the exact solutions. For the cases with variable volatility σ (that is, $\gamma \neq 0$), which implies there are no formulas to compute the exact solutions, the GLS stabilization method is applied to compute the approximated prices of an European put option. Finally, though different experiments, we find the GLS combined together with our numerical scheme gives an good numerical solutions without using very large values of N_3 when $-0.3 \leq \gamma \leq 0$, while when γ is highly positive, a similar result is achieved only by choosing the number of subintervals in $[S_b, S_\infty]$ to be sufficiently large (for example, we choose $N_3 = 2500$ to obtain a good result).

For future developments, we would like to improve our numerical scheme

to obtain a more accurate numerical solutions for the cases when γ is sufficiently large without increasing the number of subintervals in $[S_b, S_\infty]$. The fast and precise evaluation for European style option with variable and large local volatility, where no analytical solutions is known, still bear great opportunities for future numerical research.

References

[1] L.P.Franca, S. L. Frey and T. J. R. Huges. Stabilized finite element methods: I. Application to the advective-diffusive model. Compt.Meth. Appl. Mech. Engrg., 95:253-276, 1992

[2] P. V. Bochev, M. D. Gunzburger and J. N. Shadid. Stability of the SUPG Finite Element Method for Transcient Advection-Diffusion Problems. Comp. Meth. Appl. Mech. Engrg. 193: 2301-2323, 2004

[3] Y. Achdou and O. Pironneau. Computational Methods for Option Pricing. SIAM. Front. Appl. Math., 2005

[4] J. C. Cox and S. A. Ross. The Valuation of Options for Alternative Stochastic Processes. Journal of Financial Economics, 3: 145-166, 1976.